Structure−Reactivity Relationship in Interlocked Molecular Compounds and in Their Supramolecular Model Complexes†

Masumi Asakawa,‡ Christopher L. Brown,‡ Stephan Menzer,§ Françisco M. Raymo,‡ J. Fraser Stoddart,*,‡ and David J. Williams§

Contribution from the School of Chemistry, University of Birmingham, Edgbaston, Birmingham B15 2TT, U.K., and Department of Chemistry, Imperial College, South Kensington, London SW7 2AY, U.K.

Received August 21, 1996⊗

Abstract: Examination of the pseudorotaxane-like geometries adopted in the solid state by a series of 1:1 complexes revealed significant differences in the hydrogen bonding interactions between oxygen atoms in some hydroquinone-based guests carrying polyether/polyester functions and the acidic hydrogen atoms on the bipyridinium units of the host−cyclobis(paraquat-*p*-phenylene). These differences are reflected directly in the stabilities of the complexes in solution and dramatic changes in the magnitudes of their association constants (K_a values ranging from 130 to 4300 M^{-1} in MeCN at 25 °C) are observed upon varying the location of the carbonyl ester function(s) along the polyether/ester chains. A similar effect (K_a values ranging from 5 to 730 M^{-1} in Me_2CO at 25 °C) was observed in the binding of paraquat as its bipyridinium bis(hexafluorophosphate) salt by analogous macrocyclic hydroquinone-based mono- and bis-lactones. Investigations of the kinetics of hydrolyses of the ester functions revealed that−while inert in their free forms−the macrocyclic mono- and bis-lactones undergo hydrolysis when incorporated within [2]catenanes composed of one of these macrocyclic lactones and cyclobis(paraquat-*p*-phenylene). Presumably, the enhanced reactivity of the ester functions is a result of [C−H···O] hydrogen bonding interactions involving the ester carbonyl oxygen atoms and the acidic hydrogen atoms on the bipyridinium units, as suggested by single-crystal X-ray crystallographic analyses. Thus, cyclobis(paraquat-*p*-phenylene) can act as a mechanically-interlocked "catalyst".

Introduction

In recent research,[1] we have employed the tetracationic cyclophane cyclobis(paraquat-*p*-phenylene) to self-assemble[2] catenanes, rotaxanes, and pseudorotaxanes[3] incorporating hydroquinone-based polyether components. In particular, the complexes formed involving cyclobis(paraquat-*p*-phenylene) and paraquat bis(hexafluorophosphate) with acyclic and macrocyclic, respectively, hydroquinone-based compounds incorporating ester functionalities along their polyether substituents have been investigated.[4] However, the presence of ester functions within the polyether chains has a significant depressive effect on the stability of the corresponding complexes. Intrigued as we were by these observations, we envisaged the possibility of synthesizing a number of hydroquinone-based acyclic and macrocyclic polyether/ester compounds in which the position of the ester functions was varied systematically. Once prepared, we argued that these model compounds would provide us with the opportunity to investigate the effect of subtle structural changes upon (i) the efficiencies of the related self-assembly processes, (ii) the geometries in the solid and solution states, and (iii) the reactivites of the resulting molecular assemblies and supramolecular arrays. In this paper, we relate how we afforded ourselves these opportunities.

Results and Discussion

Synthesis.[5] A series of π-electron-rich hydroquinone-based acyclic compounds incorporating one carbonyl group within one or both of their two polyether chains were synthesized as shown in Schemes 1 and 2. Esterification of MEEHB with 2-(2-methoxyethoxy)acetyl chloride afforded (Scheme 1a) αCB-MEEB. Alkylation of MEEHB with 2-chloroethanol produced (Scheme 1b) MEEHEB, which was reacted with 2-methoxyacetyl chloride to give γCBMEEB. The compounds BαCMEEB and BγCMEEB were synthesized (Scheme 2, parts a and b, respectively) by esterification of 1/4DHB with 2-(2-methoxyethoxy)acetyl chloride and of BHEB with 2-methoxyacetyl chloride, respectively. The methyl esters BδCMEEB, BζCMEEEB, and BθCMEEEEB were prepared (Scheme 2c) by transesterification of the corresponding *tert*-butyl esters.

The macrocyclic bis-lactone BδCPP34C10 was synthesized (Scheme 3) by reacting the bisacid chloride of BδCHEEB with

† Molecular Meccano. 15. For part 14, see: Ashton, P. R.; Ballardini, R.; Balzani, V.; Boyd, S. E.; Credi, A.; Gandolfi, M. T.; Gómez-López, M.; Iqbal, S.; Philp, D.; Preece, J. A.; Prodi, L.; Ricketts, H. G.; Stoddart, J. F.; Tolley, M. S.; Venturi, M.; White, A. J. P.; Williams, D. J. *Chem. Eur. J.* **1997**, *3*, 146−164.

‡ University of Birmingham.

§ Imperial College.

⊗ Abstract published in *Advance ACS Abstracts*, February 15, 1997.

(1) (a) Philp, D.; Stoddart, J. F. *Synlett* **1991**, 445−458. (b) Amabilino, D. B.; Stoddart, J. F. *Pure Appl. Chem.* **1993**, *65*, 2351−2359. (c) Pasini, D.; Raymo, F. M.; Stoddart, J. F. *Gazz. Chim. It.* **1995**, *125*, 431−443. (d) Bělohradský, M.; Philp, D.; Raymo, F. M.; Stoddart J. F. in *Organic Reactivity: Physical and Biological Aspects*; Golding, B. T., Griffin, R. J., Maskill, H., Eds.; RSC Special Publication No. 148; Cambridge, U.K., 1995; pp 387−398. (e) Amabilino, D. B.; Raymo, F. M.; Stoddart, J. F. In *Comprehensive Supramolecular Chemistry*; Sauvage, J.-P., Hosseini, M. W., Eds.; Pergamon: Oxford, U.K., 1996; Vol. 9, pp 85−130.

(2) (a) Lindsey, J. S. *New J. Chem.* **1991**, *15*, 153−180. (b) Whitesides, G. M.; Mathias, J. P.; Seto, C. T. *Science* **1991**, *254*, 1312−1319. (c) Lawrence, D. S.; Jiang, T.; Levett, M. *Chem. Rev.* **1995**, *95*, 2229−2260. (d) Raymo, F. M.; Stoddart, J. F. *Curr. Opin. Colloid Interface Sci.* **1996**, *1*, 116−126. (e) Philp, D.; Stoddart J. F. *Angew. Chem., Int. Ed. Engl.* **1996**, *35*, 1154−1196.

(3) (a) Dietrich-Buchecker, C. O.; Sauvage J.-P. *Bioorg. Chem. Front.* **1991**, *2*, 195−248. (b) Gibson, H. W.; Marand, H. *Adv. Mater.* **1993**, *5*, 11−21. (c) Chambron, J. C.; Dietrich-Buchecker, C. O.; Sauvage, J.-P. *Top. Curr. Chem.* **1993**, *165*, 131−162. (d) Gibson, H. W.; Bheda, M. C.; Engen., P. T. *Prog. Polym. Sci.* **1994**, *19*, 843−945. (e) Amabilino, D. B.; Parson, I. W.; Stoddart, J. F. *Trends Polym. Sci.* **1994**, *2*, 146−152. (f) Amabilino, D. B.; Stoddart, J. F. *Chem. Rev.* **1995**, *95*, 2725−2828. (g) Bělohradský, M.; Raymo, F. M.; Stoddart, J. F. *Collect. Czech. Chem. Commun.* **1996**, *61*, 1−43. (h) Raymo, F. M.; Stoddart, J. F. *Trends Polym. Sci.* **1996**, *4*, 208−211.

(4) Asakawa, M.; Ashton, P. R.; Menzer, S.; Raymo, F. M.; Stoddart, J. F.; White, A. J. P.; Williams, D. J. *Chem. Eur. J.* **1996**, *2*, 877−893.

S0002-7863(96)02937-X CCC: $14.00

Scheme 1

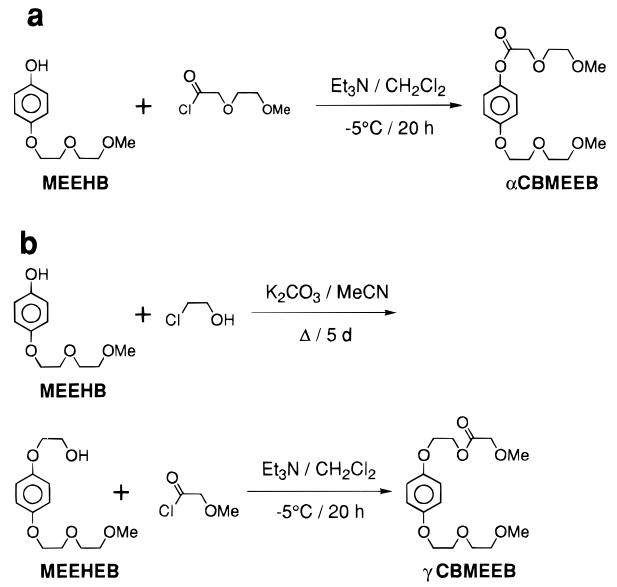

Scheme 2

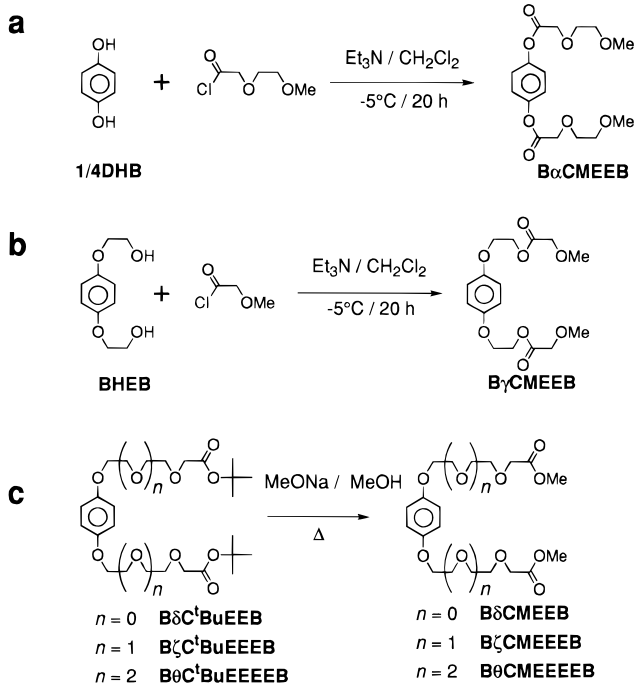

BHEEB under high-dilution conditions. Reaction (Scheme 4) of the bis(hexafluorophosphate) salt [BPYPYXY][PF_6]$_2$ with

Scheme 3

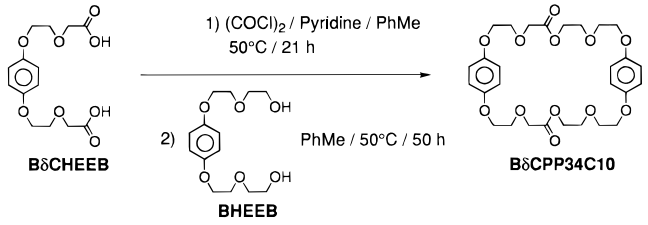

Scheme 4

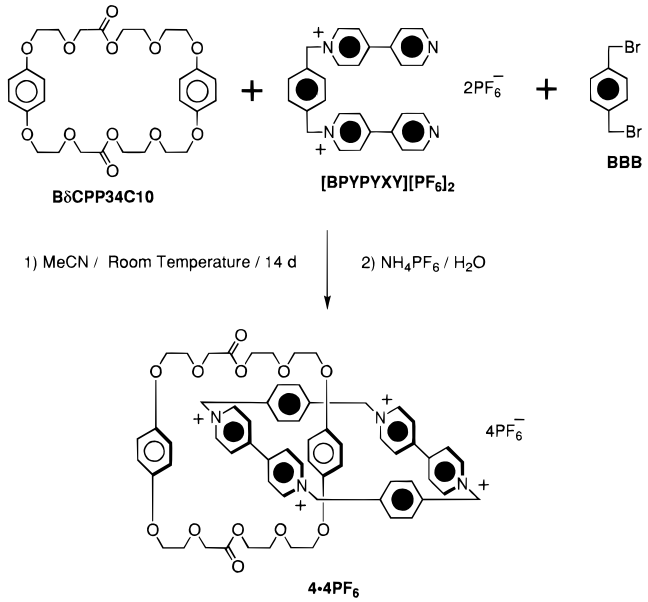

BBB in the presence of the macrocyclic bislactone BδCPP34C10 afforded the [2]catenane **4**·4PF_6, after counterion exchange.

X-ray Crystallography. The supramolecular geometries (Figures 1−5), in the solid state, of the [2]pseudorotaxanes listed in Table 1 have been deduced by single-crystal X-ray analyses. In all instances, the π-electron-rich hydroquinone ring is positioned centrally within the tetracationic cyclophane (all the superstructures have C_i symmetry) with its OC_6H_4O axis inclined by angles of tilt ranging—with one exception—between 46 and 56°. The exception is {[BαCMEEB]-[BBIPYBIXY-CY]}$^{4+}$ (Figure 2), a diphenolic diester, where the tilt angle is significantly larger at 69° and the torsional angle about the aryl carbon−oxygen bond is 70°. In addition to the normal face-to-face and T-type edge-to-face stabilizing interactions involving aromatic units, there are hydrogen bonds formed between the hydrogen atoms (H_α) in the α-positions with respect to the nitrogen atoms on the bipyridinium units and the second and third oxygen atoms O_b and O_c, respectively, along the polyether/ester chains, except when the carbonyl groups are located in

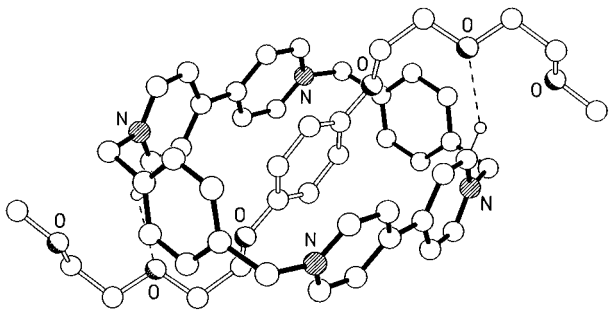

Figure 1. X-ray crystal structure of the [2]pseudorotaxane {[BMEEB]-[BBIPYBIXYCY]}$^{4+}$ showing the [C−H···O] hydrogen bonding interactions.

(5) It is convenient at this point to describe the acronyms, composed of letters and numbers, used throughout the text and in the illustrations that appear in the figures and schemes. 1,4-Dihydroxybenzene, 1,4-bis(bromomethyl)benzene, and bis(*p*-phenylene)-34-crown-10 are abbreviated to 1/4DHB, BBB, and BPP34C10, respectively. The salt, 1,1′-dimethyl-4,4′-bipyridinium hexafluorophosphate—commonly known as paraquat—is abbreviated to [PQT][PF_6]$_2$. The other acronyms can be deduced by applying the following rules. B stands for benzene when present at the end of a name and for bis when present in other parts of the name. ^{t}Bu, C, E, H, M, and P stand for *tert*-butoxy, carbonyl, ethoxy, hydroxy, methoxy, and phenoxy groups, respectively. CY, XY, BIXY, BIPY, and PYPY stand for cyclophane, xylylene, bis(xylylene), bipyridinium, and pyridylpyridinium units, respectively. The position of the carbonyl groups in the polyether chains is indicated by a Greek letter, starting from the carbon atom directly attached to the hydroquinone ring and proceeding away from it in a stepwise fashion. Numbers (*i.e.*, **1**·4PF_6, **2**·4PF_6, **3**·4PF_6, and **4**·4PF_6, respectively) are employed to indicate the [2]catenanes {[2]-[BPP34C10]-[BBIPY-BIXYCY]-catenane}[PF_6]$_4$, {[2]-[β*C*BPP34C10]-[BBIPYBIXYCY]catenane}-[PF_6]$_4$, {[2]-[B*β*CPP34C10]-[BBIPYBIXYCY]catenane}[PF_6]$_4$, and {[2]-[B*δ*CPP34C10]-[BBIPYBIXYCY]catenane}[PF_6]$_4$.

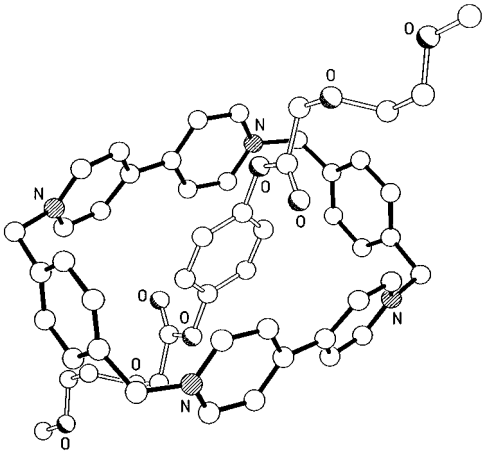

Figure 2. X-ray crystal structure of the [2]pseudorotaxane {[BαCMEEB]-[BBIPYBIXYCY]}$^{4+}$.

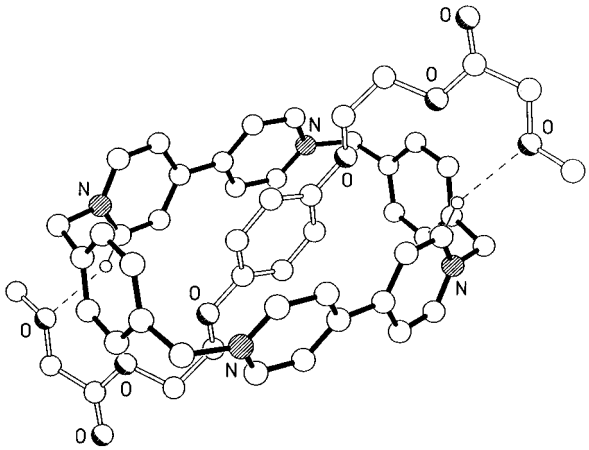

Figure 3. X-ray crystal structure of the [2]pseudorotaxane {[BγCMEEB]-[BBIPYBIXYCY]}$^{4+}$ showing the [C−H···O] hydrogen bonding interactions.

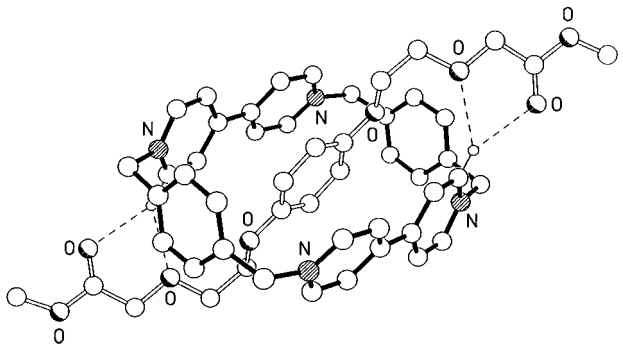

Figure 4. X-ray crystal structure of the [2]pseudorotaxane {[BδCMEEB]-[BBIPYBIXYCY]}$^{4+}$ showing the [C−H···O] hydrogen bonding interactions.

the α-positions. In {[BβCMEEB]-[BBIPYBIXYCY]}$^{4+}$ and {[BγCMEEB]-[BBIPYBIXYCY]}$^{4+}$ (Figure 3),[4] it is the oxygen atom O_c that is involved in the shortest hydrogen bonding interaction with H_α, whereas in the other pseudorotaxanes, it is O_b. In {[BαCMEEB]-[BBIPYBIXYCY]}$^{4+}$, neither O_b nor O_c are involved in hydrogen bonding.[6] When the carbonyl groups in the [2]pseudorotaxanes listed in Table 1 are located in either the β- or γ-positions (Figure 3) along the polyether/ester chains, the [O−CO−CH_2−O] linkages adopt syn-periplanar conformations in order to sustain hydrogen bonding interactions between O_c and H_α. When the carbonyl groups are moved to the α-, δ-, and θ-positions (Figures 2, 4, and 5, respectively), the more stable (*vide infra*) anti-periplanar conformation is adopted by

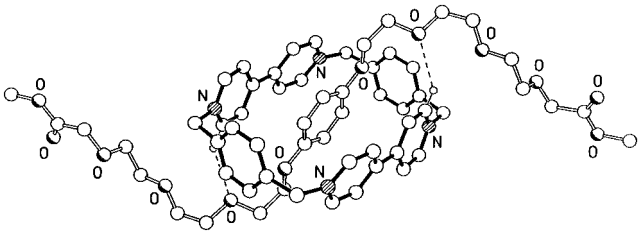

Figure 5. X-ray crystal structure of the [2]pseudorotaxane {[BθCMEEEEB]-[BBIPYBIXYCY]}$^{4+}$ showing the [C−H···O] hydrogen bonding interactions.

the [O−CO−CH_2−O] linkages. As previously observed[4] for the [2]pseudorotaxane {[BβCMEEB]-[BBIPYBIXYCY]}$^{4+}$, in the case of BγCMEEB and BθCMEEEEB, the carbonyl oxygen atoms of symmetry-related complexes form pairs of inter-complex hydrogen bonds with the hydrogen atoms H_α and H_β, respectively.

Despite the potential for two translational isomers, both of which are observed[4] in solution (*vide infra*), the single-crystal X-ray analyses of the [2]catenanes $\mathbf{3}^{4+}$ (Figure 6) and $\mathbf{4}^{4+}$ (Figure 7) revealed only the translational isomers in which the ester groups are positioned proximal to the hydroquinone ring located inside the cavity of the tetracationic cyclophane component. In $\mathbf{3}^{4+}$ and in both crystallographically-independent molecules of $\mathbf{4}^{4+}$, the mode of interlocking is very similar (Table 2) to that observed[7] in $\mathbf{1}^{4+}$, although, in $\mathbf{4}^{4+}$, the inside hydroquinone ring is displaced significantly toward the alongside bipyridinium unit, *cf.* a symmmetrical positioning in the other two [2]catenanes. In addition, in $\mathbf{3}^{4+}$ and $\mathbf{4}^{4+}$, the inside hydroquinone rings are displaced toward one of the *p*-xylyl spacers of the tetracationic cyclophane components, producing a noticeable shortening in the associated [CH···π] interactions. The OC_6H_4O axes of the inside hydroquinone rings are inclined by *ca.* 53° in $\mathbf{3}^{4+}$ and by *ca.* 45 and 48° in the two crystallographically-independent molecules of $\mathbf{4}^{4+}$ to the plane of the tetracationic cyclophane components. These tilt angles τ_i are very similar to those observed (Table 1) in the case of the related [2]pseudorotaxanes {[BβCMEEB]-[BBIPYBIXYCY]}$^{4+}$ and {[BδCMEEB]-[BBIPYBIXYCY]}$^{4+}$. In $\mathbf{3}^{4+}$, the OC_6H_4O axis of the alongside hydroquinone ring has an appreciably smaller tilt angle τ_a to the plane of the tetracationic cyclophane component than those observed in $\mathbf{4}^{4+}$, presumably as a consequence of the differencies in the [C−H···O] hydrogen bonding interactions between the hydrogen atoms H_α and the polyether/ester oxygen atoms. In contrast with $\mathbf{4}^{4+}$, where one of the ester carbonyl oxygen atoms is directed toward an H_α hydrogen atom, in $\mathbf{3}^{4+}$, both ester carbonyl groups are directed away from the plane of the tetracationic cyclophane component and are not involved in any intra-catenane hydrogen bonding interactions. However, in $\mathbf{3}^{4+}$, there are hydrogen bonding interactions between one of the H_α hydrogen atoms and the third

(6) With the exception of {[BαCMEEB]-[BBIPYBIXYCY]}$^{4+}$ and {[BδCMEEB]-[BBIPYBIXYCY]}$^{4+}$, the oxygen atoms of the carbonyl groups are involved in hydrogen bonding interactions with the hydrogen atoms H_α or H_β in the α- or β-positions, respectively, with respect to the nitrogen atoms on the bipyridinium units of the adjacent symmetry-related or lattice-related complexes. In {[BαCMEEB]-[BBIPYBIXYCY]}$^{4+}$, each carbonyl oxygen atom gives rise to intra-pseudorotaxane hydrogen bonding interactions with the two hydrogen atoms H_β of the adjacent bipyridinium unit. These interactions are responsible for the higher tilt angle τ observed in this pseudorotaxane. In {[BδCMEEB]-[BBIPYBIXYCY]}$^{4+}$, the carbonyl oxygen atoms sustain intra-pseudorotaxane hydrogen bonding interactions with the hydrogen atoms H_α.

(7) Anelli, P. L.; Ashton, P. R.; Ballardini, R.; Balzani, V.; Delgado, M.; Gandolfi, M. T.; Goodnow, T. T.; Kaifer, A. E.; Philp, D.; Pietraszkiewicz, M.; Prodi, L.; Reddington, M. V.; Slawin, A. M. Z.; Spencer, N.; Stoddart, J. F.; Vicent, C.; Williams, D. J. *J. Am. Chem. Soc.* **1992**, *114*, 193−218.

Table 1. Distances[a] (Å) and Angles[a] (deg) Characterizing the Molecular and Supramolecular Geometries of the Cyclophane {[BBIPYBIXYCY]}$^{4+}$, and the [2]Pseudorotaxanes {[BMEEB]-[BBIPYBIXYCY]}$^{4+}$, {[B(α-δ)CMEEB]-[BBIPYBIXYCY]}$^{4+}$ and {[BθCMEEEEB]-[BBIPYBIXYCY]}$^{4+}$

compound	θ	ψ	τ	$O_a\cdots N$	$O_b\cdots N$	$O_c\cdots N$	$C_\alpha\cdots O^d$	$H_\alpha\cdots O^d$	$C_\alpha H_\alpha O^d$	Z···Z′	Y···Y′	H···Y	XHY
{[BBIPYBIXYCY]}$^{4+}$ [b]	19	23								6.82	10.31		
{[BMEEB]-[BBIPYBIXYCY]}$^{4+}$	16	27	49	4.12	4.26	3.89	3.15 (O_b)	2.34 (O_b)	141 (O_b)	7.09	10.18	2.81	165
{[BαCMEEB]-[BBIPYBIXYCY]}$^{4+}$	14	30	69	5.38	7.01	8.67	*e*	*e*	*e*	7.24	10.12	2.87	152
{[BβCMEEB]-[BBIPYBIXYCY]}$^{4+}$ [c]	7	26	56	4.33	4.72	3.91	3.19 (O_c)	2.25 (O_c)	165 (O_c)	7.08	10.22	2.79	173
{[BγCMEEB]-[BBIPYBIXYCY]}$^{4+}$	17	27	46	4.03	4.51	3.95	3.23 (O_c)	2.34 (O_c)	153 (O_c)	7.10	10.25	2.88	159
{[BδCMEEB]-[BBIPYBIXYCY]}$^{4+}$	17	26	47	3.97	4.31	3.86[f]	3.30 (O_b)	2.50 (O_b)	141 (O_b)	7.05	10.21	2.82	162
{[BθCMEEEEB]-[BBIPYBIXYCY]}$^{4+}$	16	26	46	3.99	4.35	4.12	3.32 (O_b)	2.53 (O_b)	143 (O_b)	7.07	10.26	2.88	160

[a] The distances and angles indicated in the table are illustrated in the diagrams A, B, and C:

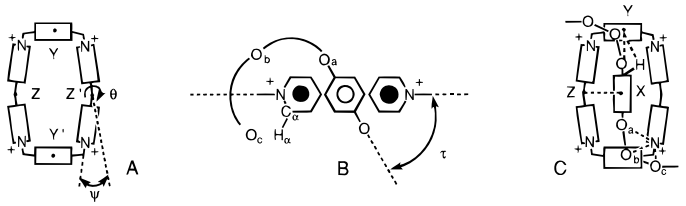

[b] The X-ray crystal structure of {[BBIPYBIXYCY]}$^{4+}$ has been reported previously in the literature (Anelli, P. L.; Ashton, P. R.; Ballardini, R.; Balzani, V.; Delgado, M.; Gandolfi, M. T.; Goodnow, T. T.; Kaifer, A. E.; Philp, D.; Pietraszkiewicz, M.; Prodi, L.; Reddington, M. V.; Slawin, A. M. Z.; Spencer, N.; Stoddart, J. F.; Vincent, C.; Williams, D. J. *J. Am. Chem. Soc.* **1992**, *114*, 193−218). [c] The X-ray crystal structure of {[BβCMEEB]-[BBIPYBIXYCY]}$^{4+}$ has been reported previously in the literature (Asakawa, M.; Ashton, P. R.; Menzer, S.; Raymo, F. M.; Stoddart, J. F.; White, A. J. P.; Williams, D. J. *Chem. Eur. J.* **1996**, *2*, 877−893). [d] The polyether oxygen atoms involved in the shortest hydrogen bonding interactions with the H_α protons are given in parentheses for each [2]pseudorotaxane. [e] In the case of {[BαCMEEB]-[BBIPYBIXYCY]}$^{4+}$, the hydrogen atoms H_α are not involved in hydrogen bonding interactions. [f] In the case of {[BδCMEEB]-[BBIPYBIXYCY]}$^{4+}$, the oxygen atoms O_c are the carbonyl oxygen atoms and are involved in hydrogen bonding interactions (lengths [$C_\alpha\cdots O$] and [$H_\alpha\cdots O$], and angle [$C_\alpha H_\alpha O$], 3.33 and 2.56 Å, and 152°, respectively) with the hydrogen atoms H_α.

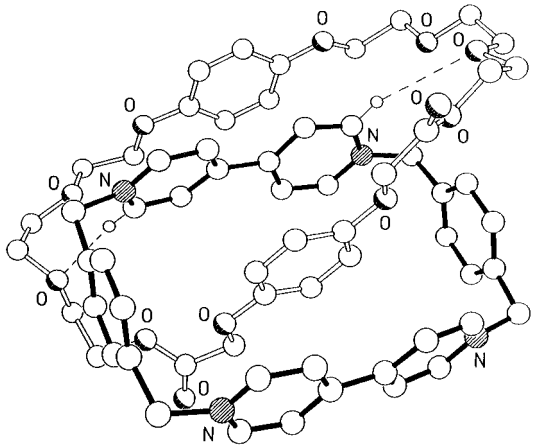

Figure 6. X-ray crystal structure of the [2]catenane **3**$^{4+}$ showing the [C−H···O] hydrogen bonding interactions.

(counting from the inside hydroquinone ring) oxygen atom of one of the polyether/ester chains (lengths [C···O] and [C−H···O], and angle [C−H···O], 3.26 and 2.31 Å, and 171°, respectively) as well as between one of the methylene hydrogen atoms of the tetracationic cyclophane component and the third (counting from the inside hydroquinone ring) oxygen atom of the opposite polyether/ester chain (lengths [C···O] and [C−H···O], and angle [C−H···O], 3.24 and 2.35 Å, and 153°, respectively). Inspection of the packing of **3**$^{4+}$ revealed that both ester carbonyl oxygen atoms are involved in pairs of [C−H···O] hydrogen bonds to the hydrogen atoms in the β-positions with respect to the nitrogen atoms on the bipyridinium units in the tetracationic cyclophane components of the centrosymmetrically-related [2]-catenane molecules. Although the molecules pack with the acceptor−donor−acceptor−donor axes co-aligned along the crystallographic *b* direction, in **3**$^{4+}$, the usual extended polar donor−acceptor stack is not formed. The space between the alongside hydroquinone ring of one [2]catenane molecule and the alongside bipyridinium unit of the next is filled by nitromethane and benzene solvent molecules. The principal difference between the two independent molecules of **4**$^{4+}$ is in the conformation of the two polyether/ester linkages. Nonetheless, in both molecules, only one of the two ester carbonyl oxygen atoms is oriented inward, facilitating hydrogen bonding with one of the H_α hydrogen atoms, while the other is directed away from any hydrogen bond donors within the [2]catenane. A consequence of the conformational differences in the polyether/ester linkage is a marked change in the relative orientations of the OC_6H_4O axes of the alongside hydroquinone rings with respect to their inside counterparts. In addition to the aforementioned hydrogen bonds to one of the ester carbonyl oxygen atoms, there are [C−H···O] hydrogen bonds from the diametrically opposite H_α hydrogen atom to the second oxygen atom (counted from the inside hydroquinone ring) of the polyether/ester linkage containing the outwardly-directed carbonyl group. These two different types of hydrogen bonding almost certainly contribute to the large twist θ_i (*ca.* 25°) between the two pyridinium rings of the inside bipyridinium units, *cf.* 13° in **3**$^{4+}$. Both crystallographically independent molecules form conventional polar donor−acceptor stacks with interstack [C−H···O] hydrogen bonds involving the outwardly-directed carbonyl groups.

Association Constants. The association constants (K_a) (Table 3) for the complexation (Figure 8) of a series of π-electron-rich hydroquinone-based guests by the bipyridinium-based cyclophane [BBIPYBIXYCY][PF_6]$_4$ were determined in CD_3CN by either ^{1}H-NMR spectroscopy or absorption spectroscopy in the visible region. The hydroquinone-based polyether BMEEB incorporating two $-CH_2CH_2O-$ ethylene linkages in each polyether chain is bound[4] strongly (K_a = 3800 M^{-1}) by the tetracationic cyclophane [BBIPYBIXYCY][PF_6]$_4$. Introduction of one ester carbonyl group into the α-, β-, or γ-position of one or both polyether chains results[4] in a decrease of the association constant of approximately 1 order of magnitude. On the contrary, the hydroquinone-based guest BδCMEEB, incorporating one ester carbonyl group in the δ-positions of both polyether/ester chains, is bound slightly more strongly with a K_a value of 1000 M^{-1}. Furthermore, introducing one or two more $-CH_2CH_2O-$ ethylene linkages within the polyether/ester chains, *i.e.* "moving" the ester groups away from

Table 2. Distances[a] (Å) and Angles[a] (deg) Characterizing the Molecular Geometries of the [2]Catenanes **1**·4PF$_6$,[b] **3**·4PF$_6$, and **4**·4PF$_6$[c]

compound	θ_i	θ_a	ψ_i	ψ_a	τ_i	τ_a	$Z_i\cdots Z_a$	$Y\cdots Y'$	$Z_a\cdots X_i$	$Z_i\cdots X_i$	$Z_i\cdots X'_a$	H···Y	XHY	H′···Y′	H′X′Y′
1·4PF$_6$	6	6	32	32	47	47	7.04	10.25	3.52	3.52	3.62	2.80	168	2.80	168
3·4PF$_6$	13	6	25	25	53	31	6.97	10.21	3.48	3.48	3.37	2.65	173	2.92	170
4a·4PF$_6$	24	3	25	27	45	64	7.06	10.25	3.48	3.55	3.54	2.81	163	3.01	152
4b·4PF$_6$	25	4	28	27	48	55	7.09	10.16	3.48	3.53	3.41	2.77	161	2.88	159

[a] The distances and angles indicated in the table are illustrated in the diagrams A, B, and C. The subscripts a and i stand for alongside and inside, respectively.

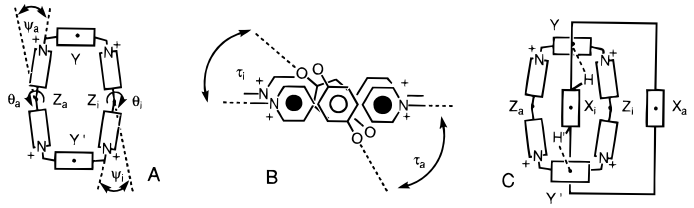

[b] The X-ray crystal structure of **1**·4PF$_6$ has been reported previously in the literature (Anelli, P. L.; Ashton, P. R.; Ballardini, R.; Balzani, V.; Delgado, M.; Gandolfi, M. T.; Goodnow, T. T.; Kaifer, A. E.; Philp, D.; Pietraszkiewicz, M.; Prodi, L.; Reddington, M. V.; Slawin, A. M. Z.; Spencer, N.; Stoddart, J. F.; Vincent, C.; Williams, D. J. *J. Am. Chem. Soc.* **1992**, *114*, 193−218). [c] Two crystallographically-independent molecules **a** and **b** are observed for **4**·4PF$_6$ in the solid state.

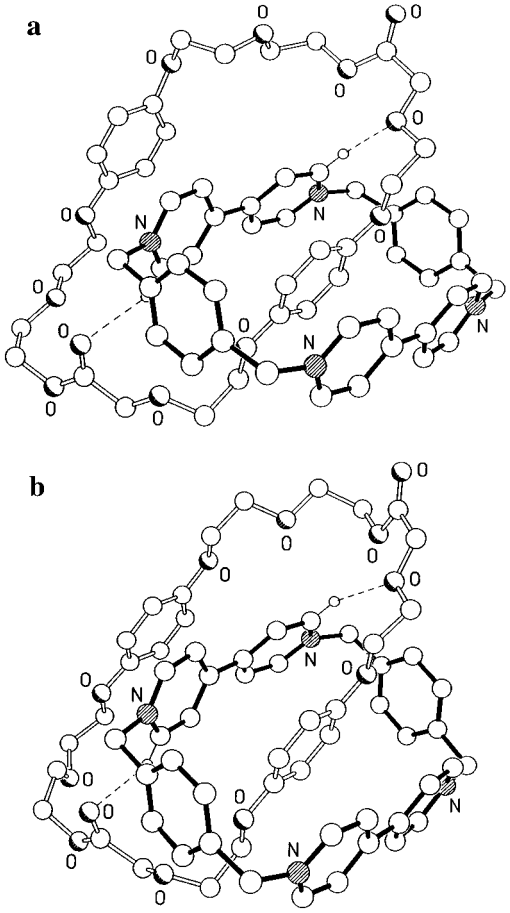

Figure 7. Two crystallographically-independent molecules (a and b) observed in the case of the [2]catenane $\mathbf{4}^{4+}$ in the crystal.

the hydroquinone ring, results in increasing the association constant up to 4300 M^{-1} in the case of the guest BθMEEEEB. These results suggest that the complexation of such hydroquinone-based guests is affected dramatically by the presence of ester functions along the polyether/ester chains. This depressive effect on binding is particularly evident when the ester carbonyl group is located in the α-, β-, and γ-positions.

In the case of the complex [BαCMEEB]-[BBIPYBIXYCY]-[PF$_6$]$_4$, the X-ray crystallographic analysis shows (Figure 2) a binding geometry significantly different from that observed for BMEEB. In both complexes, the hydroquinone ring is inserted into the cavity of the tetracationic cyclophane giving rise to

Table 3. Association Constants for the 1:1 Complexes Formed between [BBIPYBIXYCY][PF$_6$]$_4$ and the π-Electron-Rich Hydroquinone-Based Acyclic Guests at 25 °C in CD_3CN, as Well as for the 1:1 Complexes Formed between [PQT][PF$_6$]$_2$ and the π-Electron-Rich Hydroquinone-Based Macrocyclic Hosts at 25 °C in Me_2CO

compound	K_a[a] (M^{-1})	$-\Delta G°$ [b] (kcal mol^{-1})	λ_{max}[c] (nm)
BMEEB[d]	3800	4.9	455
αCBMEEB	300	3.4	350
BαCMEEB	320	3.4	380
βCBMEEB[d]	680	3.9	455
BβCMEEB[d]	520	3.7	447
γCBMEEB	430	3.7	467
BγCMEEB	130	2.9	467
BδCMEEB	1000	4.1	465
BζCMEEEB	2400	4.6	461
BθCMEEEEB	4300	5.0	468
BPP34C10[d]	730	3.9	436
βCBPP34C10[d]	73	2.5	427
BβCPP34C10[d]	5	1.0	417
BδCPP34C10	8	1.2	417

[a] The association constants (K_a) were evaluated at ^{1}H-NMR spectroscopy, employing the continuous variation methodology and UV−vis spectroscopy employing the titration methodology when the tetracationic cyclophane [BBIPYBIXYCY][PY$_6$]$_4$ was used as the host (Connors, K. A. *Binding Constants*; Wiley: New York, 1987). The protons attached to the hydroquinone ring of the guests and the charge transfer band associated with the complexes were used as the probes. UV−vis spectroscopy was employed to evaluate the association constants (K_a) by the titration methodology when [PQT][PF$_6$]$_2$ was employed as the guest, using the charge transfer band associated with the complexes as the probe. [b] Free energy ($-\Delta G°$) of complexation. [c] Wavelength (λ_{max}) corresponding to the maximum of the charge transfer band originating from the interaction between the bipyridinium units and the hydroquinone rings. [d] The values of K_a, $-\Delta G°$, and λ_{max} reported for the guests BMEEB, βCBMEEB, and BβCMEEB as well as for the hosts BPP34C10, βCBPP34C10, and BβCPP34C10 are literature values (Asakawa, M.; Ashton, P. R.; Menzer, S.; Raymo, F. M.; Stoddart, J. F.; White, A. J. P.; Williams, D. J. *Chem. Eur. J.* **1996**, *2*, 877−893).

$\pi-\pi$ stacking and edge-to-face T-type interactions. However, in the case of BαCMEEB, the hydroquinone ring is more steeply inclined with respect to the mean plane of the tetracationic cyclophane and, as a result, no hydrogen bonding stabilizing interactions between the polyether/ester oxygen atoms of BαCMEEB and the acidic protons H$_\alpha$ of [BBIPYBIXYCY]-[PF$_6$]$_4$ are observed. Presumably, in solution, a similar binding geometry is retained and the absence of hydrogen bonding stabilizing interactions accounts for the dramatic decrease in K_a for [BαCMEEB]-[BBIPYBIXYCY][PF$_6$]$_4$. Furthermore, in BαCMEEB, the ester functions are attached directly to the

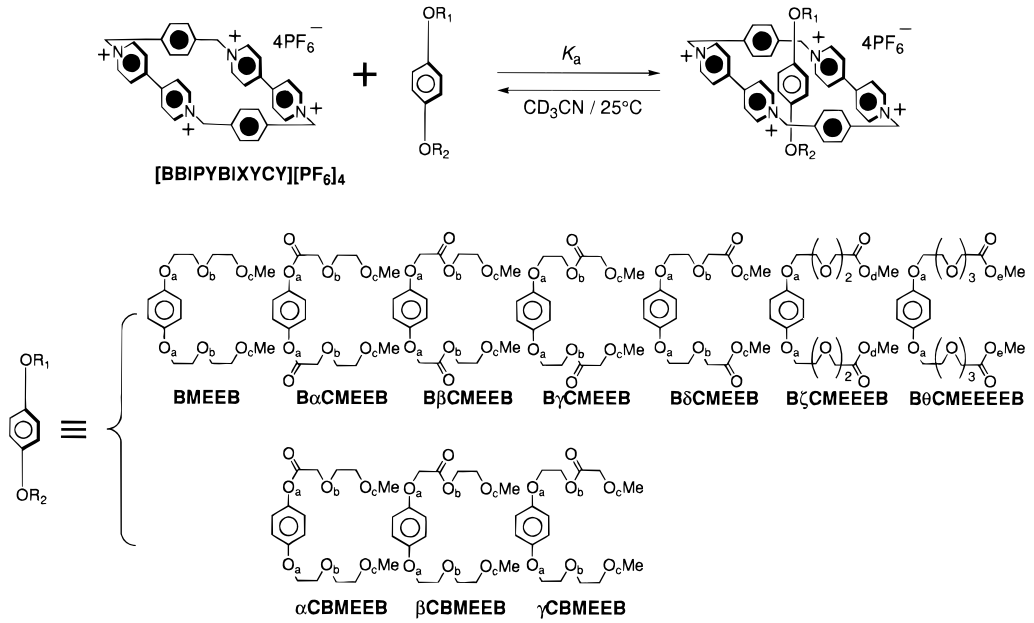

Figure 8. Complexation of the acyclic hydroquinone-based guests by the tetracationic cyclophane [BBIPYBIXYCY][PF_6]$_4$ in solution.

aromatic ring reducing its electron density and, therefore, its ability to sustain aromatic $\pi-\pi$ stacking interactions. Interestingly, the absorbance A and the wavelength λ of the charge transfer band associated with [BαCMEEB]-[BBIPYBIXYCY]-[PF_6]$_4$ ($A = 0.72$ and $\lambda = 380$ nm) are both significantly lower than in the case of [BMEEB]-[BBIPYBIXYCY][PF_6]$_4$ ($A = 0.91$ and $\lambda = 455$ nm) in MeCN at an equimolar concentration of host and guest of 10^{-3} M.

The X-ray crystallographic analysis of the complex [BMEEB]-[BBIPYBIXYCY][PF_6]$_4$ shows (Figure 1) a pair of hydrogen bonding interactions between two centrosymmetrically-related hydrogen atoms H_α in the α-positions with respect to the nitrogen atoms on the bipyridinium units and the oxygen atoms O_b (Figure 8) of the two polyether/ester chains. However, introducion of one ester carbonyl group into either the β- or the γ-positions of the polyether/ester chains reduces the electron density of O_b (*vide infra*) directing the hydrogen bonding interactions to the methoxy oxygen atoms O_c. Furthermore, the [$O_b-OC-CH_2-O_c$] linkages are forced to adopt less stable (*vide infra*) syn-periplanar conformations in order to bring O_c into close spatial proximity with the corresponding hydrogen atom H_α. In the case of the guests BδCMEEB, BζCMEEEB, and BθCMEEEEB, the electron density on the oxygen atoms O_b is restored and, within the corresponding pseudorotaxanes, hydrogen bonding interactions with the hydrogen atoms H_α are sustained by the oxygen atoms O_b, as illustrated by the X-ray crystallographic analyses (Figures 4 and 5). Furthermore, within the complexes between the tetracationic cyclophane [BBIPYBIXYCY][PF_6]$_4$ and BδCMEEB, BζCMEEEB, and BθCMEEEEB, the linkages [$O-OC-CH_2-O$] can retain more stable anti-periplanar conformations. These observations suggest that significant conformational changes of the guests BβCMEEB and BγCMEEB are required in order to achieve noncovalent bonding interactions within their corresponding complexes, comparable to those observed in the pseudorotaxanes incorporating BδCMEEB, BζCMEEEB, and BθCMEEEEB. Furthermore, such conformational changes are energetically demanding, and so, the stablilities of the corresponding complexes—*i.e.* the K_a values—are significantly lower than in the case of the other hydroquinone-based guests. The enthalpic $\Delta H°$ and entropic $T\Delta S°$ contributions (Table 4) to the free energy of binding $\Delta G°$ for the complexation of the acyclic guests BMEEB, BβCMEEB, and BγCMEEB by the tetracationic cyclophane [BBIPYBIXYCY][PF_6]$_4$ were also evaluated by measuring the temperature dependence of $\Delta G°$. In all cases, negative values of $\Delta H°$ and positive values of $T\Delta S°$ were observed. Thus, the complexation of the hydroquinone-based guests BMEEB, BβCMEEB, and BγCMEEB by the tetracationic cyclophane [BBIPYBIXYCY][PF_6]$_4$ is enthalpically driven. We believe that the cooperative noncovalent bonding interactions revealed by the X-ray crystallographic analyses are operative in solution and are responsible for the complex formation.

A similar dependence on constitution was observed for the binding (Figure 9) of [PQT][PF_6]$_2$ by hydroquinone-based macrocyclic receptors.[4] Introducing one ester carbonyl group into the β- or δ-positions within one or both of the polyether/ester chains separating the hydroquinone rings results in a dramatic decrease (Table 3) in the magnitude of the association constant. Presumably, energy-demanding conformational changes associated with the [$O-OC-CH_2-O$] linkages incorporated within the macrocyclic hosts have to be enacted in order to maximize the noncovalent bonding interactions within the complexes. Since these conformational changes are energetically demanding, they are reflected in a decrease in the binding energies present in the corresponding complexes.

^{1}H-NMR Spectroscopy. The ^{1}H-NMR spectroscopic data (δ values) for the 1:1 complexes formed between the π-electron-rich hydroquinone-based acyclic guests and the tetracationic cyclophane [BBIPYBIXYCY][PF_6]$_4$ in CD_3CN at 25 °C are listed in Table 5. The resonances associated with the hydrogen atoms H_α in the α-positions with respect to the nitrogen atoms on the bipyridinium units of the tetracationic cyclophane host are little changed[8] ($\Delta\delta$ from -0.01 to $+0.08$ ppm) upon complexation. On the contrary, as a result of the insertion of a π-electron-rich hydroquinone ring guest within the cavity of the tetracationic cyclophane host, the hydrogen atoms H_β in the β-positions with respect to the nitrogen atoms on the bipyridinium units of the host are significantly shifted. In the case of the strongly bound guests BMEEB,[4] BδCMEEB, BζCMEEEB, and BθCMEEEEB (K_a values of 3800, 1000, 2400, and 4300 M^{-1}, respectively), the resonances associated with H_β are moved significantly upfield ($\Delta\delta = -0.28$, -0.25, -0.29, and -0.30, respectively) as a consequence of shielding effects experienced by these hydrogen atoms upon complexation. In the case of

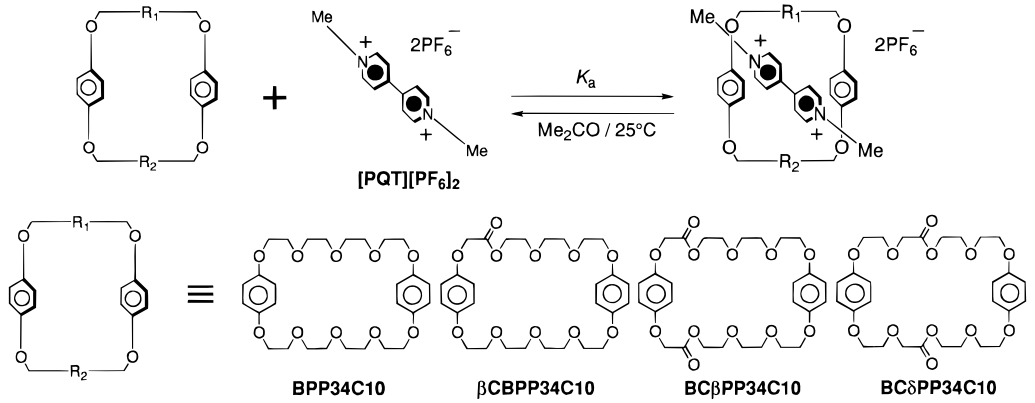

Figure 9. Complexation of $[PQT][PF_6]_2$ by the macrocyclic hydroquinone-based hosts.

Table 4. Enthalpic ($\Delta H°$) and Entropic ($T\Delta S°$) Contributions[a] to the Free Energy of Binding ($\Delta G°$) for the Complexation of the Acyclic Guests BMEEB, BβCMEEB, and BγCMEEB by the Tetracationic Cyclophane $[BBIPYBIXYCY][PF_6]_4$ in CD_3CN at 25 °C

compound	$-\Delta G°$ (kcal mol^{-1})	$-\Delta H°$ (kcal mol^{-1})	$T\Delta S°$ (kcal mol^{-1})
BMEEB	4.9	16.4	11.5
BβCMEEB	3.7	13.5	9.8
BγCMEEB	2.9	7.9	5.0

[a] The enthalpic ($\Delta H°$) and entropic ($T\Delta S°$) contributions to the free energy of binding ($\Delta G°$) were calculated from a plot of $\Delta G°$ against the temperature T. The values of $\Delta G°$ at different temperatures were determined from the association constants measured at the corresponding T values.

the less stable complexes between $[BBIPYBIXYCY][PF_6]_4$ and the acyclic guests incorporating one ester carbonyl group in the α-, β-, or γ-positions of both polyether chains (K_a values of 320, 520, and 130 M^{-1}, respectively),[4] the resonances associated with H_β are weakly affected ($\Delta\delta = -0.01$, -0.04, and -0.04, respectively). Interestingly, when the guests αCBMEEB, βCBMEEB,[4] and γCBMEEB (K_a values of 300, 680, and 430 M^{-1}, respectively) incorporating one ester carbonyl group within only one of the two polyether/ester chains are employed, $\Delta\delta$ values ($\Delta\delta = -0.08$, -0.10, and -0.16, respectively) higher than those observed for the related guests incorporating two ester groups are observed in keeping with the trend in the K_a values.

Table 5. ^{1}H-NMR Spectroscopic Data (δ Values) for the Complexes and Reference Compounds in CD_3CN at 25 °C

compound	polycationic component H_α[a]	polycationic component H_β[b]	neutral component ArH[c]
$[BBIPYBIXYCY][PF_6]_4$[d]	8.89	8.17	
BMEEB[d]			6.85
[BMEEB]-$[BBIPYBIXYCY][PF_6]_4$[d]	8.91	7.89	4.49
αCBMEEB[e]			7.00
[αCBMEEB]-$[BBIPYBIXYCY][PF_6]_4$[e]	8.90	8.05	6.05
BαCMEEB			7.18
[BαCMEEB]-$[BBIPYBIXYCY][PF_6]_4$	8.88	8.16	6.94
βCBMEEB[d]			6.85
[βCBMEEB]-$[BBIPYBIXYCY][PF_6]_4$[d]	8.89	8.07	5.45
BβCMEEB[d]			6.85
[BβCMEEB]-$[BBIPYBIXYCY][PF_6]_4$[d]	8.89	8.13	6.36
γCBMEEB			6.85
[γCBMEEB]-$[BBIPYBIXYCY][PF_6]_4$	8.90	8.01	5.28
BγCMEEB			6.85
[BγCMEEB]-$[BBIPYBIXYCY][PF_6]_4$	8.87	8.13	6.38
BδCMEEB			6.85
[BδCMEEB]-$[BBIPYBIXYCY][PF_6]_4$	8.97	7.92	4.68
BζCMEEEB			6.85
[BζCMEEEB]-$[BBIPYBIXYCY][PF_6]_4$	8.92	7.88	4.42
BθCMEEEEB			6.85
[BθCMEEEEB]-$[BBIPYBIXYCY][PF_6]_4$	8.92	7.87	4.06
$[PQT][PF_6]_2$[d]	8.84	8.36	
BPP34C10[d]			6.73
[BPP34C10]-$[PQT][PF_6]_2$[d]	8.80	8.07	6.44
βCBPP34C10[d]			6.77
[βCBPP34C10]-$[PQT][PF_6]_2$[d]	8.83	8.32	6.71
BβCPP34C10[d,f]			6.79, 6.78
[BβCPP34C10]-$[PQT][PF_6]_2$[d,f]	8.84	8.36	6.77, 6.76
BδCPP34C10[f]			6.77, 6.75
[BδCPP34C10]-$[PQT][PF_6]_2$[f]	8.84	8.35	6.75, 6.74

[a] Protons attached to the bipyridinium units in the α-positions with respect to the nitrogen atoms. [b] Protons attached to the bipyridinium units in the β-positions with respect to the nitrogen atoms. [c] Protons attached to the hydroquinone rings incorporated within the π-electron-rich components. [d] Literature values (Asakawa, M.; Ashton, P. R.; Menzer, S.; Raymo, F. M.; Stoddart, J. F.; White, A. J. P.; Williams, D. J. *Chem. Eur. J.* **1996**, *2*, 877−893). [e] The π-electron-rich acyclic compound αCBMEEB incorporates one hydroquinone ring which gives rise, in the ^{1}H-NMR spectrum, to an AA′BB′ system centered on the δ value listed in the table. [f] The π-electron-rich macrocycles BβCPP34C10 and BδCPP34C10 incorporate two hydroquinone rings, each giving rise to a singlet in the ^{1}H-NMR spectrum.

(8) These observations are not in conflict with the existence of [C−H···O] hydrogen bonding interactions between the polyether oxygen atoms and the hydrogen atoms H_α within the pseudorotaxane-like complexes and the [2]catenanes in solution. Only two out of a total of eight H_α hydrogen atoms are involved simultaneously in [C−H···O] hydrogen bonding interactions in each case. Nonetheless, only one doublet is observed in the ^{1}H-NMR spectrum for all the eight protons H_α as a result of exchange processes which are fast on the ^{1}H-NMR time scale. Thus, the observed chemical shifts for the protons H_α are averaged values—*i.e.*, the deshielding effect caused by the [C−H···O] hydrogen bonding interactions is "diluted" considerably. The dynamic processes responsible for the site exchange of the eight protons H_α are (i) equilibration between complex and "free" host and guest, (ii) tilting of the O···O axis of the hydroquinone ring located inside the cavity of the tetracationic cyclophane with respect to the N···N axes of the sandwiching bipyridinium units—a process termed "rocking" (see: Anelli, P. L.; Ashton, P. R.; Ballardini, R.; Balzani, V.; Delgado, M.; Gandolfi, M. T.; Goodnow, T. T.; Kaifer, A. E.; Philp, D.; Pietraszkiewicz, M.; Prodi, L.; Reddington, M. V.; Slawin, A. M. Z.; Spencer, N.; Stoddart, J. F.; Vicent, C.; Williams, D. J. *J. Am. Chem. Soc.* **1992**, *114*, 193−218), and (iii) circumrotation of the tetracationic cyclophane with respect to the O···O axis of the "inside" hydroquinone ring, in the case of the pseudorotaxane-like complexes, and (i) circumrotation of the tetracationic cyclophane through the cavity of the macrocyclic lactone, (ii) circumrotation of the macrocyclic lactone through the cavity of the tetracationic cyclophane, as well as (iii) "rocking", in the case of the [2]catenanes. The ^{1}H-NMR spectrum of the complex [BMEEB]-$[BBIPYBIXYCY][PF_6]_4$ recorded in CD_3COCD_3 at 190 K—*i.e.*, the lowest practical temperature in this solvent—shows only one doublet for all the eight protons H_α, suggesting that the dynamic processes are still fast on the ^{1}H-NMR time scale at this temperature. On the contrary, in the case of the [2]catenane **1**·4PF_6, the exchange processes are slow on the ^{1}H-NMR time scale in CD_3COCD_3 at 190 K. As a result, two equally intense partially overlapped resonances are observed for the protons H_α of the bipyridinium unit located "alongside" the cavity of the macrocyclic polyether in addition to two resonances of equal intensities separated by a difference in chemical shift of $\Delta\delta$ 0.18 for the protons H_α of the "inside" bipyridinium unit. The larger difference between the δ values of the resonances associated with the "inside" bipyridinium unit is, presumably, a consequence of the [C−H···O] hydrogen bonding interactions which involve only one of the two pairs of protons H_α.

Similarly, the hydrogen atoms ArH attached to the hydroquinone rings experience a dramatic upfield shift upon complexation as a result of the shielding effect exerted by the sandwiching bipyridinium units of the host. In the complexes incorporating BMEEB, BδCMEEB, BζCMEEEB, and BθCMEEEEB, the resonances associated with ArH are shifted by $\Delta\delta$ values of −2.36, −2.17, −2.43, and −2.79 ppm, respectively. When the guests BαCMEEB, BβCMEEB, and BγCMEEB are employed, the hydroquinone ring resonances are shifted by $\Delta\delta$ values of only −0.24, −0.49, and −0.47 ppm, respectively. In the case of the guests αCBMEEB, βCBMEEB, and γCBMEEB incorporating only one ester carbonyl group in one of the two polyether/ester chains, the hydroquinone ring resonances are more significantly shifted ($\Delta\delta$ = −0.95, −1.40, and −1.57 ppm, respectively) than in the case of the related guests incorporating two ester carbonyl groups, once again in keeping with the trend in the K_a values.

A similar effect is observed (Table 5) for the complexation of $[PQT][PF_6]_2$ by the hydroquinone-based macrocyclic polyethers. When the macrocyclic polyether BPP34C10 is employed, the hydrogen atoms H_α and H_β of $[PQT][PF_6]_2$, as well as the hydroquinone hydrogen atoms (ArH), are shifted upfield ($\Delta\delta$ = −0.04, −0.29, and −0.29 ppm, respectively). However, when the macrocyclic lactones βCBPP34C10, BβCPP34C10, and BδCPP34C10 are employed, very small chemical shift changes are observed in the resonances associated with H_α, H_β, and ArH, reflecting the low K_a values associated with these complexes.

The asymmetry of the π-electron-rich macrocyclic components of the [2]catenanes listed in Table 6, induced by the presence of one or two ester carbonyl groups in the β- or δ-positions of one or both polyether/ester chains, gives rise to the existence of two translational isomers for each [2]catenane in solution. However, the circumrotation of the π-electron-rich macrocyclic component through the cavity of the tetracationic cyclophane component is fast on the ^{1}H-NMR time scale at room temperature. As a result, the two translational isomers of each [2]catenane are in fast exchange at room temperature and sharp averaged resonances are observed in the ^{1}H-NMR spectra. On cooling solutions of the [2]catenanes down to −50 °C, the dynamic processes become slow on the ^{1}H-NMR time scale and two sets of signals, arising separately from each of the translational isomers, can be detected in the ^{1}H-NMR spectrum. Integration of these resonances affords the ratios between the translational isomers, which correspond to 4:1, 10:1, and 4:1 for **2**·4PF_6,[4] **3**·4PF_6,[4] and **4**·4PF_6, respectively. As suggested by the X-ray crystallographic analyses of the [2]-catenanes, **3**·4PF_6 (Figure 8) and **4**·4PF_6 (Figure 9), in all cases, the major isomer in solution is believed to be the one bearing the ester carbonyl group(s) proximal to the hydroquinone ring located inside the cavity of the tetracationic cyclophane component. This isomer preference is presumably a result of more favorable intercomponent hydrogen bonding interactions (*vide supra*) involving the oxygen atoms of the ester carbonyl groups. By employing the coalescence methodology,[9] the free energies of activation for the site exchange processes involving the interconversion of the two translational isomers were evaluated and are listed in Table 6.

Kinetic Studies. The X-ray crystallographic analysis of the [2]catenane **4**·4PF_6 revealed (Figure 7) a hydrogen bonding interaction between the oxygen atom of one of the two ester carbonyl groups incorporated within the π-electron-rich macrocyclic polyether component and one of the hydrogen atoms H_α in the α-positions with respect to the nitrogen atoms on the bipyridinium units of the tetracationic cyclophane component. As a result of such a hydrogen bonding interaction, the electrophilic character of the carbon atom of the related ester carbonyl group is increased, and so, enhanced hydrolysis of the ester function is expected within the [2]catenane. In order to support this observation, each of the macrocyclic lactones βCBPP34C10, BβCPP34C10, and BδCPP34C10 was heated at 50 °C in a 1:1 mixture of D_2O and CD_3CN and the reactions were followed by ^{1}H-NMR spectroscopy. However, the ^{1}H-NMR spectra recorded after 7 days did not reveal any significant difference from the spectra recorded at the outset of the experiment—*i.e.*, the ester functions are not hydrolyzed under these conditions. Even when the same experiments were repeated, after adding 1 mol equiv of either $[PQT][PF_6]_2$ or $[BBIPYBIXYCY][PF_6]_4$ to the reaction mixtures, the macrocyclic lactones were recovered unaltered after 7 days. However, by contrast, treating (Figure 10) the [2]catenanes, **2**·4PF_6, **3**·4PF_6, and **4**·4PF_6, under the same conditions—namely, 50 °C in a 1:1 mixture of D_2O and CD_3CN—hydrolyses of the macrocyclic lactones incorporated within the [2]catenanes occur. The plots of the relative concentration of the [2]catenanes, calculated by integrating the resonances associated with the hydrogen atoms H_α against time are shown in Figure 11. Interestingly, after approximately 800 h, an equilibrium between reagent and products is reached in all three processes. Fur-

Table 6. Free Energies of Activation for the Dynamic Processes Associated with the [2]Catenanes **2**·4PF_6, **3**·4PF_6, and **4**·PF_6 in Solution

compound	$\Delta G^{\ddagger}_{(A\rightarrow B)}$[a] (kcal mol^{-1})	$\Delta G^{\ddagger}_{(B\rightarrow A)}$[a] (kcal mol^{-1})	T_c[b] (K)
2·4PF_6[c,d]	15.1	13.8	307
3·4PF_6[c,e]	15.5	14.7	295
4·4PF_6[e]	15.5	14.8	304

[a] Free energy of activation ($\Delta G^{\ddagger}_{(A\rightarrow B)}$) for the interconversion of the translational isomer A into B (see diagram below) at the coalescence temperature. Free energy of activation ($\Delta G^{\ddagger}_{(B\rightarrow A)}$) for the interconversion of the translational isomer B into A at the coalescence temperature. The free energies values were determined by employing eqs 3 and 4 using the hydrogen atoms [CH_2CO] of the methylene group(s) attached to the ester carbonyl group(s) as the probes.

$$\Delta G^{\ddagger}_{(A\rightarrow B)} = RT_c(23.759) - \frac{k_{(A\rightarrow B)}}{T_c} \quad (3)$$

$$\Delta G^{\ddagger}_{(B\rightarrow A)} = RT_c(23.759) - \frac{k_{(B\rightarrow A)}}{T_c} \quad (4)$$

The rate constants ($k_{(A\rightarrow B)}$) and ($k_{(A\rightarrow B)}$) associated with the interconversion of the translational isomer A into B and *vice versa* were determined by employing eqs 5 and 6, where P_A and P_B are the populations of the translational isomers A and B, respectively, and $\Delta\nu$ is the frequency difference (Oki, M. *Applications of Dynamic NMR Spectroscopy to Organic Chemistry*; VCH: Weinheim, Germany, 1985).

$$k_{(A\rightarrow B)} = 2\pi P_B \Delta\nu \quad (5)$$

$$k_{(B\rightarrow A)} = 2\pi P_A \Delta\nu \quad (6)$$

[b] Coalescence temperature, T_c. [c] Literature values (Asakawa, M.; Ashton, P. R.; Menzer, S.; Raymo, F. M.; Stoddart, J. F.; White, A. J. P.; Williams, D. J. *Chem. Eur. J.* **1996**, *2*, 877−893). [d] In CD_3COCD_3. [e] In CD_3COCD_3/CD_3CN (7:3, v/v).

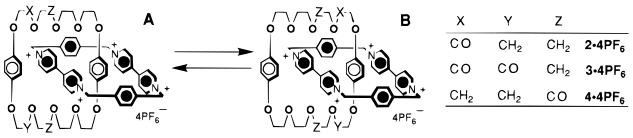

(9) (a) Sutherland, I. O. *Ann. Rep. NMR Spectrosc.* **1971**, *4*, 71−235. (b) Sandström, J. *Dynamic NMR Spectroscopy*; Academic Press: London, 1982. (c) Oki M. *Applications of Dynamic NMR Spectroscopy to Organic Chemistry*; VCH: Weinheim, Germany, 1985.

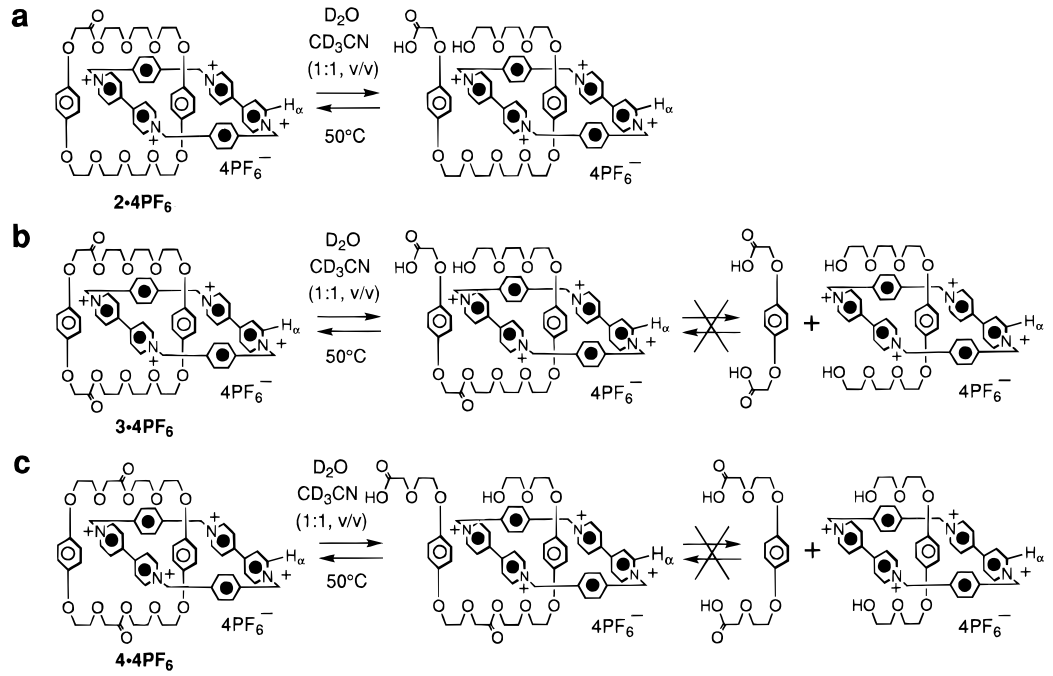

Figure 10. Hydrolysis of the [2]catenanes (a) **2**·4PF$_6$, (b) **3**·4PF$_6$, and (c) **4**·4PF$_6$.

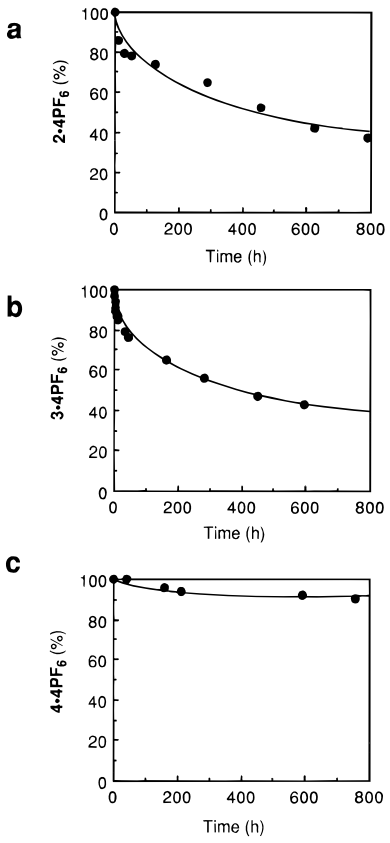

Figure 11. Plots of the relative concentrations of the [2]catenanes (a) **2**·4PF$_6$, (b) **3**·4PF$_6$, and (c) **4**·4PF$_6$ against time.

thermore, in the case of the bis-lactones incorporated within **3**·4PF$_6$ and **4**·4PF$_6$, only *one* of the two ester groups is hydrolyzed. The HPLC chromatogram (Figure 12d) of the reaction mixture of the [2]catenane **4**·4PF$_6$—recorded after 800 h, that is, at equilibrium—shows only three peaks. These peaks correspond to (i) the [2]catenane (Figure 12a), (ii) the tetracationic cyclophane [BIBIPYBIXYCY][PF$_6$]$_4$ (Figure 12b), and (iii) the acyclic carboxylic acid BβCHEHEEEPEEEEB produced as a result of the hydrolysis of only *one* ester group. None of the compound BHEEEB (Figure 12c), which should be formed

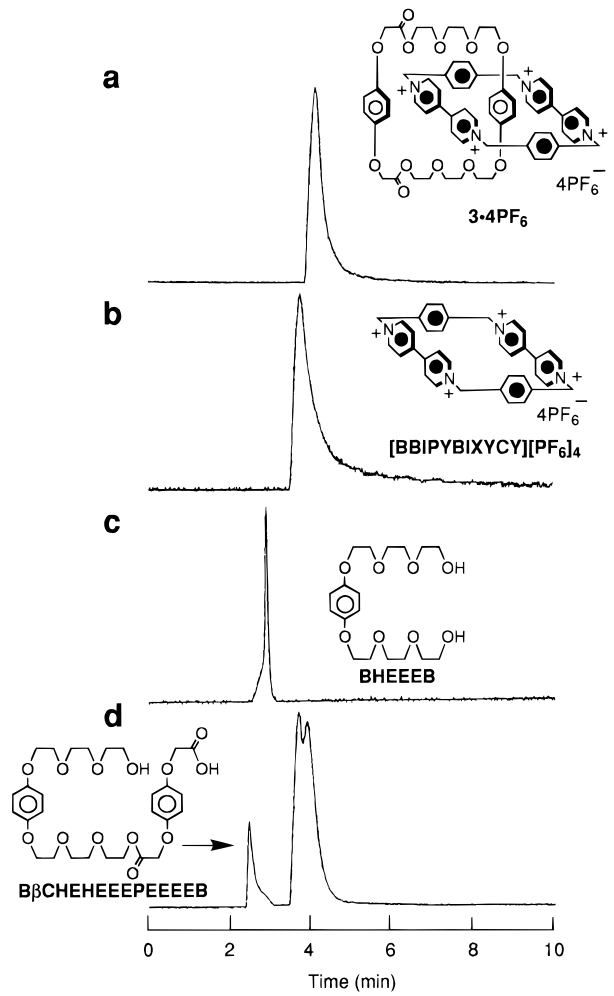

Figure 12. HPLC charts of (a) **3**·4PF$_6$, (b) the tetracationic cyclophane [BBIPBIXYCY][PF$_6$]$_4$, (c) the diol BHEEEB, and (d) the carboxylic acid BβCHEHEEEPEEEEB.

after the hydrolysis of the second ester group, is detected in the reaction mixture. By employing a nonlinear curve-fitting program, the kinetic and thermodynamic parameters listed in

Table 7. Kinetic and Thermodynamic Parameters for the Hydrolysis of the [2]Catenanes **2**·4PF_6, **3**·4PF_6, and **4**·4PF_6 in D_2O/CD_3CN (1:1, v/v) at 50 °C

compound	$k_{\rightarrow}$[a] (s^{-1})	$k_{\leftarrow}$[b] (s^{-1})	$\Delta G^{\ddagger}_{\rightarrow}$[c] (kcal mol^{-1})	$\Delta G^{\ddagger}_{\leftarrow}$[d] (kcal mol^{-1})	K_{eq}[e]	$\Delta G°$[f] (kcal mol^{-1})
2·4PF_6	6.7×10^{-7}	3.7×10^{-7}	28.1	28.5	1.8	−0.4
3·4PF_6	7.9×10^{-7}	4.0×10^{-7}	28.0	28.4	2.0	−0.4
4·4PF_6	8.6×10^{-8}	7.6×10^{-7}	29.4	28.0	0.1	1.4

[a] Rate constant ($k_{\rightarrow}$) for the forward reaction, *i.e.* hydrolysis of the catenane. [b] Rate constant ($k_{\leftarrow}$) for the backward reaction, *i.e.* macrocyclization. [c] Free energy of activation ($\Delta G^{\ddagger}_{\rightarrow}$) for the forward reaction, *i.e.* hydrolysis of the catenane. [d] Free energy of activation ($\Delta G^{\ddagger}_{\leftarrow}$) for the backward reaction, *i.e.* macrocyclization. [e] Equilibrium constant (K_{eq}). [f] Free energy of equilibrium ($\Delta G°$).

Table 8. Parameters Associated with the Electrostatic Interactions[a] Occurring between the Acidic Hydrogen Atoms H_α of the Cyclophane [BBIPYBIXYCY][PF_6]$_4$ and the Polyether/ester Oxygen Atoms of the Hydroquinone-Based Guests BMEEB, BβCMEEB, BγCMEEB, and BδCMEEB within the Corresponding [2]Pseudorotaxanes

	O_a			O_b			O_c		
compound	$-i_a$[b]	$O_a\cdots H_\alpha$[c] (Å)	$-R_a$[d] ($Å^{-1}$)	$-i_b$[b]	$O_b\cdots H_\alpha$[c] (Å)	$-R_b$[d] ($Å^{-1}$)	$-i_c$[b]	$O_c\cdots H_\alpha$[c] (Å)	$-R_c$[d] ($Å^{-1}$)
BMEEB	66.5	3.20	20.8	74.0	2.23	33.2	70.0	2.42	28.9
BβCMEEB	61.1	3.74	16.3	65.9	2.90	22.7	72.0	2.14	33.6
BγCMEEB	57.0	3.21	17.8	61.0	2.74	22.3	64.0	2.36	27.1
BδCMEEB	61.9	3.23	19.2	69.7	2.39	29.2	72.8[e]	2.32[e]	31.4[e]

[a] The electrostatic interactions occurring between the hydrogen atoms H_α of [BBIPYBIXYCY][PF_6]$_4$ and the polyether/ester oxygen atoms of the guests within the [2]pseudorotaxanes are schematically illustrated in the diagram. [b] Relative intensities of the electrostatic potential mapped on to the total electron density surface for the oxygen atoms O_a, O_b, and O_c, as generated with the program Spartan Version 4.1 (Spartan Version 4.1, Wavefunction Inc., 1995). [c] Distance between H_α and O_a, O_b, and O_c. [d] Ratio between i and the corresponding distance [O···H_α]. This term is proportional to the electrostatic contribution to the energy associated with the interaction occurring between O and H_α. The monotonic correlation between the sum of R_a, R_b, and R_c and the binding energy is illustrated in the plot. [e] In the case of the guest BδCMEEB, O_c is the carbonyl oxygen atom.

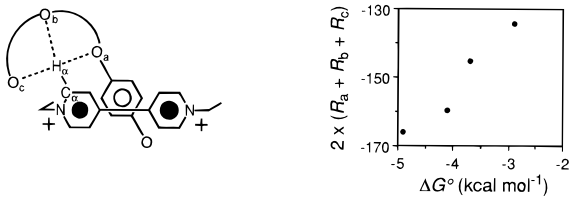

Table 7 were determined from the plots shown in Figure 11. Interestingly, little difference is observed between the parameters associated with the [2]catenanes incorporating the macrocyclic lactones βCBPP34C10 and BβCPP34C10 comprising one ester carbonyl group in the β-position of one and both polyether chains, respectively. On the contrary, the rate constant for the hydrolysis of the [2]catenane, incorporating the macrocyclic bis-lactone BδCPP34C10 possessing one ester carbonyl group in the δ-positions of both polyether chains, is approximately 1 order of magnitude lower. These results suggest that within the mechanically-interlocked compounds—namely, the [2]-catenanes—the tetracationic cyclophane acts as a "Lewis acid", increasing the reactivity of the ester function(s) present within the macrocyclic lactones as a result of hydrogen bonding interactions. Furthermore, the difference in the rate of hydrolysis observed on "moving" the ester carbonyl groups from the β- to the δ-positions along the polyether/ester chains suggests that the strength of the hydrogen bonds is related to the location of the ester carbonyl groups within the polyether/ester chains.[10]

The potential enanchment of reactivity of the ester functions incorporated within the acyclic hydroquinone-based compounds B(α-δ)MEEB, BζMEEEB, and BθMEEEEB, upon complex formation with the tetracationic cyclophane [BBIPYBIXYCY][PF_6]$_4$, was also investigated. However, when equimolar amounts of [BBIPYBIXYCY][PF_6]$_4$ and any of the acyclic guests were treated in a 1:1 mixture of D_2O and CD_3CN 50 °C—*i.e.*, the conditions employed to hydrolyze the [2]-catenanes—no hydrolysis of the guests was observed at all. These observations suggest that the tetracationic cyclophane [BBIPYBIXYCY][PF_6]$_4$ acts only as a "Lewis acid" only when it is mechanically-interlocked within [2]catenanes and not when it is complexed within [2]pseudorotaxanes. Presumably, in solution within the pseudorotaxane-like, complexes the oxygen atoms of the ester carbonyl groups are not involved in any hydrogen bonding interactions with the tetracationic cyclophane, as was indeed revealed by X-ray crystallography (*vide supra*) in the solid state.

Molecular Modeling. In order to gain further insight into the reasons for the differences in the binding energies of the pseudorotaxane-like complexes, the structures of the hydroquinone-based polyether/esters BMEEB, BβCMEEB, BγCMEEB, and BδCMEEB, obtained from the X-ray crystallographic analyses, were subjected to a single-point semiempirical treatment employing[11] the AM1 Hamiltonian to calculate the relative intensities of the electrostatic potential mapped on to the total electron density surface of these molecules. The maximum values i_a, i_b, and i_c for the relative intensities of the electrostatic potential which we have mapped out on to the total electron density surface for the oxygen atoms O_a, O_b, and O_c, respectively, together with the distances [$O_a\cdots H_\alpha$], [$O_b\cdots H_\alpha$], and [$O_c\cdots H_\alpha$] between O_a, O_b, and O_c, respectively, and the

(10) The X-ray crystallographic analysis of the [2]catenane **3**·4PF_6 revealed that the carbonyl oxygen atoms of the ester functions are involved in pairs of intermolecular hydrogen bonding interactions, rather than intramolecular ones, as in the case of **4**·4PF_6. Nonetheless, the rate of hydrolysis of the macrocyclic bis-lactone component is faster in the case of **3**·4PF_6. Presumably, the intramolecular hydrogen bonding interactions responsible for the enhanced reactivity of the ester function in solution are over-ruled in the solid state by more favorable intermolecular hydrogen bonding interactions.

(11) Spartan V 4.1, Wavefunction, Inc., 18401 Von Karman Ave., #370 Irvine, CA 92715.

hydrogen atom H_α closest to them in the case of BMEEB, BβCMEEB, BγCMEEB, and BδCMEEB, are listed in Table 8. The ratios R_a, R_b, and R_c between i_a, i_b, and i_c and the corresponding distances [$O_a\cdots H_\alpha$], [$O_b\cdots H_\alpha$], and [$O_c\cdots H_\alpha$], respectively, are proportional[12] to the attractive electrostatic contribution to the energy associated with the interactions occurring between the corresponding oxygen atom and the proximal H_α. The sum of R_a, R_b, and R_c provides an estimate of the total attractive electrostatic contribution to the [$O\cdots H_\alpha$] interactions for a single polyether/ester chain (twice the value of $R_a + R_b + R_c$ yields the total attractive electrostatic contribution for both polyether/ester chains) and its monotonic correlation with the binding energy (Table 8) corroborates the observations suggested by the X-ray analyses—*i.e.*, subtle stereoelectronic changes induced by varying the location of the carbonyl groups along the polyether/ester chains are reflected in the stabilities of the 1:1 complexes as a result of modifications to the geometries of the hydrogen bonding interactions between the polyether/ester oxygen atoms and the bipyridinium hydrogen atoms H_α.

X-ray crystallographic analyses of the pseudorotaxane-like complexes formed between the guests BδCMEEB, BζCMEEEB, and BθCMEEEEB and the tetracationic cyclophane [BBIPYBIXYCY][PF_6]$_4$ revealed (*vide supra*) anti-periplanar conformations for the [O−OC−CH_2−O] linkages. On the contrary, in the case of the complexes incorporating the guests BβCMEEB and BγCMEEB, the [O−OC−CH_2−O] linkages adopt syn-periplanar conformations. Ab initio calculations on the model compound, methyl 2-methoxyacetate, revealed (Table 9) energy differences favoring of the anti-periplanar conformation—*i.e.*, the anti-periplanar conformation (A) is more stable than the syn-periplanar one (B)—presumably, as a result of a stereoelectronic effect.[13] Thus, in the case of the guests BβCMEEB and BγCMEEB, the change of the conformation of the [O−OC−CH_2−O] linkages of each polyether/ester chain from the more stable anti- to the syn-periplanar conformation is required in order to achieve favorable hydrogen bonding interactions between the polyether oxygen atoms and the bipyridinium hydrogen atoms upon complexation. Furthermore, examination (Table 9) of the electrostatic iso-surfaces of the anti- and syn-periplanar conformation of methyl 2-methoxyacetate revealed an electrostatic potential surface of the anti-periplanar conformation A approximately twice as large as the one for the syn-periplanar conformation B—*i.e.*, the anti-periplanar conformation is a better hydrogen bond acceptor.[14] These observations are consistent with the values for the association constants (Table 3) of the pseudorotaxane-like complexes. Low K_a values are observed for the complexes [BβCMEEB][BBIPYBIXYCY]-[PF_6]$_4$ and [BγCMEEB][BBIPYBI-XYCY][PF_6]$_4$ in which the [O−OC−CH_2−O] linkages of the polyether/ester chains adopt the "less hydrogen bond accepting" syn-periplanar conformation.

Table 9. Calculated Potential Energy Difference between the Anti-periplanar and the Syn-periplanar Conformations of Methyl 2-Methoxyacetate in the Gas Phase

method	$-\Delta E^a$ kcal mol^{-1})
AM1	6.4
PM3	4.6
3-21G*/HF	0.9
3-21G*/MP2	1.2

[a] Potential energy difference between the anti-periplanar A and syn-periplanar B conformations calculated by employing the program Spartan Version 4.1 (Spartan Version 4.1, Wavefunction Inc., 1995). Electrostatic iso-surfaces of A and B are shown below.

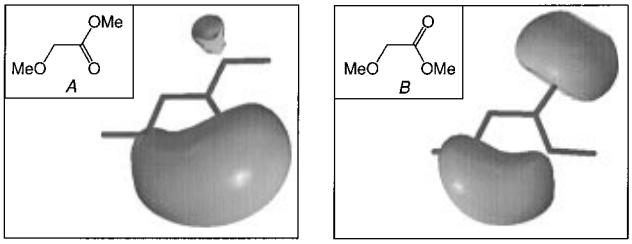

Conclusions

The tetracationic cyclophane cyclobis(paraquat-*p*-phenylene) binds acyclic hydroquinone-based polyethers with pseudorotaxane-like geometries in solution and in the solid state. However, subtle structural changes to the guests—namely, the introduction of one ester function along one or both polyether chains—affect significantly the stereoelectronic match between the receptor and the substrate. As a consequence, the stabilities of the complexes are greatly affected in solution. Moreover, varying the location of the ester function(s) along the polyether/ester chains results in dramatic changes in the association constants. X-ray crystallographic analyses of the pseudorotaxanes demonstrated the geometries adopted by these complexes in the solid state and has revealed hydrogen bonding interactions between the polyether/ester oxygen atoms and the acidic hydrogen atoms of the tetracationic cyclophane. However, the geometries associated with hydrogen bonding interactions are influenced markedly by the positions of the ester carbonyl groups. As confirmed by molecular modeling studies, the ester oxygen atom [CH_2−O−CO] adjacent to the carbonyl group is a weaker hydrogen bonding donor than an ether oxygen atom [CH_2−O−CH_2]. Furthermore, in order to achieve such hydrogen bonding interactions, substantial changes in conformations, involving torsional angles associated with [OCH_2−COO] linkages, are required. As a result, the position of the ester carbonyl group determines the stability and the geometry of the complex. A similar effect was observed upon complexation of paraquat bis(hexafluorophosphate) by macrocyclic hydroquinone-based mono- and bis-lactones. These macrocycles have also been incorporated within mechanically-interlocked compounds, along with cyclobis(paraquat-*p*-phenylene), to afford [2]catenanes. Again, the hydrogen bonding interactions existing between the acidic hydrogen atoms of the the bipyridinium units and the oxygen atoms of the ester functions are responsible for control-

(12) The electrostatic energy V associated with the attractive interaction between two point charges q and q' of opposite sign, separated by a distance r, is given by eq 1, where ϵ_m is the permittivity of the medium—*i.e.*, a

$$V = \frac{q'}{4\pi\epsilon_m}\frac{q}{r} \quad (1)$$

measure of its ability to transmit an electric field (Isaacs, N. S. *Physical Organic Chemistry*; Longman: Harlow, 1995). When the point charge q' is constant, the electrostatic energy V is function of the ratio between q and r. The values of i_a, i_b, and i_c associated with the oxygen atoms O_a, O_b, and O_c reported in Table 8 are proportional to the charge density at the same point on the electron density surface—*i.e.*, they are proportional to q. As the tetracationic host is the same in all the complexes, the i value for the bipyridinium hydrogen atoms H_α in the various complexes can be considered constant—*i.e.*, it is proportional to q'. Similarly, the interactomic distance [$O\cdots H_\alpha$] can be used in (1) as the r value. As a result, the attractive electrostatic contribution to any [$O\cdots H_\alpha$] interaction is proportional to the ratio between the i value of O and the [$O\cdots H_\alpha$] distance.

(13) For a discussion on the conformational analysis of 1,2-dimethoxyethane in the gas and solution phases, see: Williams, D. J.; Hall, K. B. *J. Phys. Chem.* **1996**, *100*, 8224−8229.

(14) This effect is reminicent of the different basicity observed for syn and anti lone pairs of carboxylates, see: (a) Zimmerman, S. C.; Cramer, K. D. *J. Am. Chem. Soc.* **1988**, *110*, 5906−5908. (b) Huff, J. B.; Askew, B.; Duff, R. J.; Rebek, J., Jr. *J. Am. Chem. Soc.* **1988**, *110*, 5908−5909. (c) Li, Y.; Houk, K. N. *J. Am. Chem. Soc.* **1989**, *111*, 4505−4507. (d) Huff, J. B.; Tadayoni, B. M.; Rebek, J., Jr. *J. Am. Chem. Soc.* **1991**, *113*, 2247−2253.

ling the translational isomerism associated with the [2]catenanes and the reactivites of their ester functions. The electrophilicities of the ester carbon atoms are greatly enhanced as a result of these noncovalent bonding interactions. The inertness toward hydrolysis of the macrocyclic lactones in their free forms compares with their reactivities when incorporated within the [2]catenanes. In addition, kinetic studies have demonstrated that the rate of hydrolysis changes upon varying the position of the ester carbonyl groups, *i.e.* by varying the geometries of the hydrogen bonding interactions.

Experimental Section

General Methods. Chemicals were purchased from Aldrich and used as received. Solvents were dried [MeCN (from P_2O_5), CH_2Cl_2 (from CaH_2), and PhMe (from CaH_2)], according to procedures described in the literature.[15] MEEHB,[4] BδC^{t}BuEEB,[16] BζC^{t}BuEEEB, BθC^{t}BuEEEEB,[16] BδCHEEB,[16] BHEEB,[7] BMEEB,[4] βCBMEEB,[4] BβCMEEB,[4] [BBIPYXY][PF_6]$_2$,[7] βCBPP34C10,[4] BβCBP34C10,[4] **2**·4PF_6,[4] and **3**·4PF_6[4] were all prepared according to literature procedures. Thin layer chromatography (TLC) was carried out using aluminum sheets precoated with silica gel 60 F (Merck 5554). The plates were inspected by UV light and developed with iodine vapor. Column chromatography was carried out using silica gel 60 F (Merck 9385, 230−400 mesh). High-performance liquid chromatography (HPLC) was carried out on a Gilson 714 system, fitted with a UV detector. Melting points were determined on an Electrothermal 9200 apparatus and are not corrected. Elemental analyses were performed by the University of Sheffield Microanalytical Service. Low-resolution mass spectra were performed using a Kratos profile spectrometer operating in electron impact (EIMS) mode. Fast atom bombardment mass spectra (FABMS) were recorded on a Kratos MS80 spectrometer operating at 8 keV using a xenon primary atom beam. The matrix used was 3-nitrobenzyl alcohol (NOBA). UV−vis spectra were recorded on a Perkin-Elmer Lambda 2 using HPLC quality solvents. ^{1}H-NMR spectra were recorded on either a Bruker AC300 (300 MHz) spectrometer or a Bruker AMX400 (400 MHz) spectrometer using either the solvent or TMS as internal standards. ^{13}C-NMR spectra were recorded on either a Bruker AC300 (75.5 MHz) spectrometer or a Bruker AMX400 (100.6 MHz) spectrometer using either the solvent or TMS as internal standards. All chemical shifts are quoted in ppm on the δ scale, and the coupling constants are expressed in hertz (Hz).

2-(2-Methoxyethoxy)acetyl Chloride. 2-(2-Methoxyethoxy)acetic acid (14.1 g, 100 mmol) was added to a mixture of dry PhMe (100 mL) and pyridine (3 drops). Oxalyl chloride (25.4 g, 127 mmol) was added at room temperature, and the reaction mixture was stirred for 24 h. The solution was filtered through Celite, and the solvent was evaporated in vacuo to give 2-(2-methoxyethoxy)acetyl chloride as a yellow oil (13.2 g, 86%), which was employed in the following step without further purification: ^{1}H-NMR ($CDCl_3$) δ 4.48 (2H, s), 3.77−3.74 (2H, m), 3.58−3.55 (2H, m), 3.36 (3H, s); ^{13}C-NMR ($CDCl_3$) δ 172.0, 76.6, 71.9, 71.3, 59.0.

1-[2-(2-Methoxyethoxy)ethoxy]-4-[[2-methoxyethoxy)methylene]-carboxy]benzene (αCBMEEB). A solution of 2-(2-methoxyethoxy)-acetyl chloride (15.0 g, 98.3 mmol) in dry CH_2Cl_2 (50 mL) was added at −5 °C over 1 h to a vigorously stirred solution of MEEHB (9.70 g, 45.7 mmol) and Et_3N (5.60 g, 55.3 mmol) in dry CH_2Cl_2 (100 mL). The stirring was continued for 20 h during which time the temperature rose gradually to room temperature. Thereafter, the solution was poured into ice−water (200 mL). The organic phase was washed with a saturated aqueous solution (200 mL) of $NaHCO_3$ and dried (Na_2SO_4). The evaporation of the solvent in vacuo afforded αCBMEEB as a pale yellow oil (13.5 g, 90%): EIMS *m/z* 328 $[M]^+$; ^{1}H-NMR ($CDCl_3$) δ 7.07−7.02 (2H, m), 6.98−6.93 (2H, m), 4.35 (2H, s), 4.11−4.08 (2H, m), 3.78−3.75 (2H, m), 3.73−3.70 (2H, m), 3.64−3.61 (2H, m), 3.55−3.49 (4H, m), 3.32 (3H, s), 3.30 (3H, s); ^{13}C-NMR ($CDCl_3$) δ 170.6, 157.7, 145.0, 123.5, 116.2, 72.6, 72.6, 71.5, 71.2, 70.3, 69.1, 68.9, 58.9. Anal. Calcd for $C_{16}H_{24}O_7$: C, 58.53; H, 7.37. Found: C, 58.54; H, 7.42.

1-[2-(2-Methoxyethoxy)ethoxy]-4-(2-hydroxyethoxy)benzene (MEE-HEB). MEEHB (14.0 g, 67.0 mmol) was added to a suspension of K_2CO_3 (46.0 g, 335 mmol) in dry MeCN (200 mL) under N_2. The suspension was stirred vigorously for 30 min at 70 °C, and a solution of 2-chloroethanol (12.1 g, 150 mmol) in MeCN (100 mL) was added over 1 h. The resulting reaction mixture was heated under reflux for 5 days. After the mixture was cooled to room temperature, the suspension was filtered and the solid was washed with MeCN (200 mL). The combined organic solutions were concentrated in vacuo, and the residue was dissolved in CH_2Cl_2 (200 mL) and washed with H_2O (3 × 100 mL). The organic phase was dried with Na_2SO_4, and the solvent was evaporated in vacuo. Purification of the residue by column chromatography (SiO_2, $MeCO_2Et/CH_2Cl_2$, 1:20) gave MEEHEB as a yellow oil (1.6 g, 9.4%): FABMS *m/z* 256 $[M]^+$; ^{1}H-NMR ($CDCl_3$) δ 6.84 (4H, s), 4.10−4.07 (2H, m), 4.03−4.00 (2H, m), 3.93−3.90 (2H, m), 3.85−3.82 (2H, m), 3.72−3.69 (2H, m), 3.59−3.56 (2H, m), 3.38 (3H, s), 2.12 (1H, br s); ^{13}C-NMR ($CDCl_3$) δ 153.1, 153.0, 115.7, 115.5, 71.9, 70.6, 70.0, 69.8, 68.0, 61.3, 59.0.

1-[2-(2-Methoxyethoxy)ethoxy]-4-[2-[(methoxymethylene)carboxy]-ethoxy]benzene (γCBMEEB). A solution of 2-methoxyacetyl chloride (670 mg, 5.90 mmol) in dry CH_2Cl_2 (50 mL) was added at −5 °C over 1 h to a vigorously stirred solution of MEEHEB (1.00 g, 45.7 mmol) and Et_3N (660 mg, 6.5 mmol) in dry CH_2Cl_2 (100 mL). The stirring was continued for 20 h during which time the temperature rose gradually to room temperature. Thereafter, the solution was poured into ice−water (200 mL). The organic phase was washed with a saturated aqueous solution (200 mL) of $NaHCO_3$ and dried (Na_2SO_4). The evaporation of the solvent in vacuo afforded a residue which was purified by column chromatography (SiO_2, $MeCO_2Et/CH_2Cl_2$, 1:30) to give γCBMEEB as a yellow oil (940 mg, 74%): EIMS *m/z* 328 $[M]^+$; ^{1}H-NMR (CD_3CN) δ 6.87 (4H, s), 4.43−4.40 (2H, m), 4.16−4.13 (2H, m), 4.05−4.02 (2H, m), 4.03 (2H, s), 3.777−3.74 (2H, m), 3.63−3.60 (2H, m), 3.50−3.47 (2H, m), 3.37 (3H, s), 3.31 (3H, s); ^{13}C-NMR (CD_3CN) δ 171.2, 154.4, 153.8, 116.7, 116.5, 72.7, 71.2, 70.2, 69.0, 67.6, 63.9, 59.4, 58.9. Anal. Calcd for $C_{16}H_{24}O_7$: C, 58.53; H, 7.37. Found: C, 58.62; H, 7.24.

1,4-Bis[[(2-methoxyethoxy)methylene]carboxy]benzene (BαCMEEB). A solution of 2-(2-methoxyethoxy)acetyl chloride (13.0 g, 85.2 mmol) in dry CH_2Cl_2 (50 mL) was added at −5 °C over 30 min to a vigorously stirred solution of 1/4DHB (4.6 g, 42.0 mmol) and Et_3N (8.69 g, 55.2 mmol) in dry CH_2Cl_2 (100 mL). The stirring was continued for 15 h, during which time the temperature raised gradually to room temperature and then the solution was poured into ice−water (300 mL). The organic phase was washed with a saturated aqueous solution of $NaHCO_3$ (200 mL) and dried (Na_2SO_4). The solent was removed in vacuo, and the purification of the residue by recrystallization from hexane/CH_2Cl_2 gave BαCMEEB as a crystalline white solid (13.7 g, 95%): mp 96−97 °C; FABMS *m/z* 342 $[M]^+$; ^{1}H-NMR ($CDCl_3$) δ 7.13 (4H, s), 4.40 (4H, s), 3.83−3.80 (4H, m), 3.62−3.59 (4H, m), 3.40 (6H, s); ^{13}C-NMR ($CDCl_3$) δ 168.8, 147.7, 122.3, 72.0, 71.1, 68.7, 59.0. Anal. Calcd for $C_{16}H_{22}O_8$: C, 56.14; H, 6.48. Found: C, 55.81; H, 6.23.

1,4-Bis[2-[(methoxymethylene)carboxy]ethoxy]benzene (BγCMEEB). A solution of methoxyacetyl chloride (5.00 g, 46.1 mmol) in dry CH_2Cl_2 (30 mL) was added at −5 °C over 30 min to a vigorously stirred solution of BHEB (3.00 g, 15.4 mmol) and Et_3N (5.10 g, 50.7 mmol) in dry CH_2Cl_2 (100 mL) and dry THF (150 mL). The stirring was continued for 20 h, during which time the temperature rose gradually to room temperature. Thereafter, the solution was poured into ice−water (200 mL). The organic phase was washed with a saturated aqueous solution of $NaHCO_3$ (200 mL) and dried with Na_2SO_4. The evaporation of the solvent in vacuo afforded a residue which was purified by column chromatography (SiO_2, $MeCO_2Et/CH_2Cl_2$, 1:5). Crystallization of the residue from hexane/CH_2Cl_2 gave BγCMEEB as a white crystalline solid (2.7 g, 52%): mp 61−63 °C; FABMS *m/z* 342 $[M]^+$; ^{1}H-NMR ($CDCl_3$) δ 6.85 (4H, s), 4.53−4.49 (4H, m), 4.17−4.13 (4H, m), 4.09 (4H, s), 3.46 (6H, s); ^{13}C-NMR ($CDCl_3$) δ 170.2, 153.0, 115.8, 69.7, 66.5, 63.2, 59.4. Anal. Calcd for $C_{16}H_{22}O_8$: C, 56.14; H, 6.48. Found: C, 56.17; H, 6.53.

(15) Furniss, B. S.; Hannaford, A. J.; Smith, P. W. G.; Tatchell, A. R. *Practical Organic Chemistry*; Longman: New York, 1989.

(16) Asakawa, M.; Ashton, P. R.; Brown, G. R.; Hayes, W.; Menzer, S.; Stoddart, J.F.; White, A. J. P.; Williams, D. J. *Adv. Mater.* **1996**, *1*, 37−41.

Table 10. Crystal Data, Collection, and Refinement Parameters for the [2]Pseudorotaxanes Incorporating the π-Electron-Deficient Cyclophane [BBIPYBIXYCY][PF_6]$_4$ and the π-Electron-Rich Acyclic Compounds Listed in Turn

data	BMEEB	BαCMEEB	BβCMEEB	BγCMEEB	BδCMEEB	BθCMEEEEB
formula·4PF_6	$C_{52}H_{58}N_4O_6$	$C_{52}H_{54}N_4O_8$	$C_{52}H_{54}N_4O_8$	$C_{52}H_{54}N_4O_8$	$C_{52}H_{54}N_4O_8$	$C_{60}H_{70}N_4O_{12}$
solvent	2MeCN	4MeCN	4MeCN·0.5H_2O	H_2O	3.5MeCN	
formula weight	1497.0	1607.1	1615.1	1460.9	1586.6	1619.1
lattice type	triclinic	monoclinic	triclinic	triclinic	triclinic	triclinic
space group	$P\bar{1}$	$P2_1/n$	$P\bar{1}$	$P\bar{1}$	$P\bar{1}$	$P\bar{1}$
T (K)	293	293	293	293	293	293
cell dimensions						
a (Å)	11.566(2)	15.376(6)	10.785(2)	11.007(2)	11.037(1)	11.736(3)
b (Å)	12.556(3)	11.337(3)	13.497(3)	12.226(2)	13.861(1)	12.417(3)
c (Å)	13.901(4)	20.772(6)	13.975(2)	13.471(2)	14.174(1)	13.909(4)
α (deg)	110.95(2)		91.61(2)	88.83(2)	77.672(3)	100.71(2)
β (deg)	92.33(2)	90.51(1)	103.19(1)	70.13(1)	72.146(7)	106.75(2)
γ (deg)	113.87(2)		110.33(1)	66.70(1)	76.014(7)	110.65(2)
V (Å^3)	1683.0(7)	3621.0(2)	1836.4(6)	1552.1(4)	1979.9(3)	1720.2(7)
Z	1[a]	2[a]	1[a]	1[a]	1[a]	1[a]
D_c (g cm^{-3})	1.477	1.474	1.460	1.563	1.331	1.563
F(000)	766	1644	826	744	811	830
μ (mm^{-1})	2.104	2.029	2.008	2.294	1.846	2.166
θ range (deg)	3.5−55.0	3.6−58.0	3.3−55.0	3.5−55.0	3.3−55.0	3.5−60.0
no. of unique reflns						
measd	4231	5028	4620	3901	4768	5103
obsd[b]	3126	4166	3468	3009	3449	4098
no. of variables	495	556	523	470	481	470
R_1 (%)	6.77	6.64	8.70	8.73	14.70	8.41
wR_2 (%)	17.25	18.61	24.02	24.87	40.24	22.23
a, b[c]	0.096, 2.258	0.102, 3.890	0.146, 3.264	0.130, 4.622	0.313, 5.144	0.086, 6.049

[a] The molecule has crystallographic C_i symmetry. [b] $|F_o| > 4\sigma(|F_o|)$. [c] Weighting factors.

1,4-Bis[2-[(methoxycarbonyl)methoxy]ethoxy]benzene (BδCMEEB). BδC^{t}BuEEB (1.09 g, 2.60 mmol) was added to a solution of Na (1.0 mg, 0.04 mmol) in MeOH (100 mL), and the solution was heated under reflux for 2 h. After the mixture was cooled to room temperature, the solvent was evaporated in vacuo. Purification of the residue by column chromatography (SiO_2, $MeCO_2Et/CH_2Cl_2$, 1:30) gave BδCMEEB as a white solid (710 mg, 80%): EIMS *m/z* 342 [M]$^+$; ^{1}H NMR ($CDCl_3$) δ 6.85 (4H, s), 4.16 (4H, s), 4.08−4.05 (4H, m), 3.83−3.81 (4H, m), 3.68 (6H, s); ^{13}C NMR ($CDCl_3$) δ 171.7, 154.1, 116.5, 70.8, 69.1, 68.9, 52.2. Anal. Calcd for $C_{16}H_{22}O_8$: C, 56.14; H, 6.48. Found: C, 56.23; H, 6.52.

1,4-Bis[2-[2-[(methoxycarbonyl)methoxy]ethoxy]ethoxy]-benzene (BζCMEEEB). BζCBMEEEB was obtained as a clear oil (0.29 g, 89%) from the *tert*-butyl diester BζC^{t}BuEEEB (0.302 g, 0.75 mmol) by employing a procedure identical to that used for the preparation of BδCMEEB: FABMS *m/z* 430 [M]$^+$; ^{1}H NMR ($CDCl_3$) δ 3.67−3.71 (14H, m), 3.75−3.80 (4H, m), 3.99−4.04 (4H, m), 4.12 (4H, s), 6.77 (4H, s); ^{13}C NMR ($CDCl_3$) δ 51.7, 67.9, 68.6, 69.8, 70.7, 70.9, 115.5, 153.0, 170.9. Anal. Calcd for $C_{20}H_{30}O_{10}$: C, 55.81; H, 7.03. Found: C, 55.66; H, 6.97.

1,4-Bis[2-[2-[2-[(methoxycarbonyl)methoxy]ethoxy]ethoxy]ethoxy]-benzene (BθCBMEEEEB). BθCBMEEEEB was obtained as a clear oil (0.28 g, 85%) from the *tert*-butyl diester BθCB^{t}BuEEEEB (0.315 g, 0.64 mmol) by employing a procedure identical to that used for the preparation of BδCBMEEB: FABMS *m/z* 518 [M]$^+$; ^{1}H NMR ($CDCl_3$) δ 3.61−3.72 (22H, m), 3.76−3.81 (4H, m), 4.00−4.05 (4H, m), 4.12 (4H, s), 6.80 (4H, s); ^{13}C NMR ($CDCl_3$) δ 51.7, 68.1, 68.6, 69.9, 70.6, 70.7, 70.9, 115.6, 153.1, 168.1, 170.9. Anal. Calcd for $C_{24}H_{38}O_{12}$: C, 55.59; H, 7.39. Found: C, 55.71; H, 7.43.

1,4,7,10,13,18,21,24,27,30-Decaoxa-6,25-dioxo[13,13]-paracyclophane (BδCPP34C10). BδCBHEEB (4.40 g, 14.0 mmol) was suspended in a mixture of dry PhMe (200 mL) and dry pyridine (3 drops). Oxalyl chloride (14.2 g, 112 mmol) was added at room temperature and under N_2 to the suspension. The temperature was raised to 50 °C and stirring maintained for 21 h. After the mixture was cooled to room temperature, the solution was concentrated to give a yellow solid, which was redissolved in dry PhMe (250 mL). The PhMe solution of the bis-acid chloride and a solution of BHEEB (2.86 g, 10.0 mmol) in dry PhMe (250 mL) were added over 2 h and 30 min, from two separate dropping funnels, to vigorously stirred dry PhMe (500 mL) mantained at 50 °C under N_2. The stirring was continued for 48 h, and then the solution was concentrated in vacuo. Purification of the residue by column chromatography (SiO_2, hexane/Me_2CO, 6:4) gave a solid, which was recrystallized from hexane/Me_2CO (6:4) to give BδCPP34C10 as a crystalline white solid (760 mg, 14%): mp 88 °C; FABMS *m/z* 564 [M]$^+$; ^{1}H NMR (CD_3CN) δ 6.78 (4H, s), 6.75 (4H, s), 4.28−4.25 (4H, m), 4.15 (4H, s), 3.99−3.95 (8H, m), 3.80−3.70 (12H, m); ^{13}C NMR (CD_3CN) δ 171.3, 154.1, 153.9, 116.5, 116.4, 70.6, 70.4, 69.7, 69.6, 69.0, 64.7. Anal. Calcd for $C_{28}H_{36}O_{12}$: C, 59.57; H, 6.43. Found: C, 59.46; H, 6.27.

{**[2]-[BδCPP34C10]-[BBIPYBIXYCY]catenane**}**[PF_6]$_4$ (4·4PF_6).** A solution of BδCPP34C10 (198 mg, 0.350 mmol), [BPYPYXY][PF_6]$_2$ (742 mg, 1.05 mmol), BBB (360 mg, 1.37 mmol), and NaI (3 mg, 21.0 μmol) in dry DMF (20 mL) was stirred at room temperature for 14 days. The solvent was removed in vacuo, and the resulting solid residue was purified by column chromatography (SiO_2, MeOH/2 M NH_4Cl/$MeNO_2$, 7:2:1) to afford **4**·4PF_6, after counterion exchange, as a red crystalline solid (332 mg, 57%): mp 295 °C (dec); FABMS *m/z* 1665 [M]$^+$, 1519 [M − PF_6]$^+$, 1374 [M − 2PF_6]$^+$, 1229 [M − 3PF_6]$^+$; ^{1}H NMR (CD_3COCD_3/CD_3CN, 7:3, v/v) δ 9.16 (8H, d, J = 7 Hz), 8.03 (8H, d, J = 7 Hz), 7.97 (8H, s), 5.95 (8H, s), 4.65 (4H, br s), 4.46 (4H, br s), 3.90 (8H, br s), 3.78−3.75 (8H, m), 3.67−3.65 (4H, m); ^{13}C NMR (CD_3COCD_3/CD_3CN, 7:3, v/v) δ 147.2, 145.5, 137.6, 131.8, 126.6, 115.8, 114.0, 70.8, 70.3, 68.3, 65.7, 64.5. Anal. Calcd for $C_{64}H_{68}F_{24}N_4O_{12}P_4$: C, 46.17; H, 4.12; N, 3.37. Found: C, 46.30; H, 4.06; N, 3.35.

X-ray Crystallography. In the case of the [2]pseudorotaxanes and of the [2]catenane **4**·4PF_6, single crystals suitable for X-ray crystallographic analysis were grown by vapor diffusion of *i*-Pr_2O into a MeCN solution of the compound. In the case of the [2]catenane **3**·4PF_6, single crystals suitable for X-ray crystallographic analysis were grown by vapor diffusion of benzene into a $MeNO_2$ solution of the [2]catenane. X-ray diffraction measurements were performed on either a Siemens P4/PC or a Siemens P4/PC RA instruments using Cu Kα radiation (λ = 1.541 78 Å) and ω-scans. The data were corrected for Lorentz and polarization factors but not for absorption. The structures were solved by direct methods and refined by full-matrix least-squares based F^2, using the SHELXTL package version 5.0.[17] Hydrogen atoms were placed in calculated postions (C−H distance 0.96 Å) and assigned isotropic thermal parameters [U(H) = 1.2 U_{eq}(C) and for methyl groups U(H) = 1.5 U_{eq}(C)]. The crystal data and the data collection and

(17) Sheldrick, G. M. SHELXTL Version 5.0, Siemens Analytical X-ray Instruments Inc., 1994.

Table 11. Crystal Data, Collection, and Refinement Parameters for the [2]Catenanes **3**·4PF_6 and **4**·4PF_6

data	**3**·4PF_6	**4**·4PF_6
formula·4PF_6	$C_{64}H_{68}N_4O_{12}$	$C_{64}H_{68}N_4O_{12}$
solvent	PhH·5.5$MeNO_2$·0.5H_2O	2MeCN
formula weight	2087.96	1747.2
lattice type	triclinic	monoclinic
space group	$P\bar{1}$	$P2_1/c$
T (K)	198	203
cell dimensions		
a (Å)	13.865(1)	39.907(3)
b (Å)	18.057(1)	14.011(1)
c (Å)	19.865(3)	27.333(4)
α (deg)	90.11(1)	
β (deg)	104.51(1)	98.52(1)
γ (deg)	98.52(1)	
V (Å^3)	4757.9	15114(1)
Z	2	8[a]
D_c (g cm^{-3})	1.460	1.536
F(000)	2150	7168
μ (mm^{-1})	1.81	2.028
θ range (deg)	2.3−55.0	2.3−58.0
no. of unique reflns		
measd	11825	21036
obsd[b]	8182	13254
no. of variables	1267	2053
R_1 (%)	9.91	9.09
wR_2 (%)	26.94	22.57
a, b[c]	0.197, 12.969	0.123, 41.203

[a] There are two crystallographically independent molecules. [b] $|F_o| > 4\sigma(|F_o|)$. [c] Weighting factors.

refinement parameters are listed in Tables 10 and 11. In the case of the [2]pseudorotaxane [Bδ MEEB]-[BBIPYBIXYCY][PF_6]$_4$, 3.5 MeCN solvent molecules are disordered in eight positions. All full-weight non-hydrogen atoms were refined anisotropically. In the case of the [2]pseudorotaxanes [BMEEB]-[BBIPYBIXYCY][PF_6]$_4$, [Bγ MEEB]-[BBIPYBIXYCY][PF_6]$_4$, and [Bα MEEB]-[BBIPYBIXYCY][PF_6]$_4$, the disorder observed in the hexafluorophosphate counterions was resolved by refining the counterions in two orientations with reduced occupancy. All non-hydrogen atoms were refined anisotropically. In the case of the [2]catenane **3**·4PF_6, the hexafluorophosphate counterions were located in five positions, four in general positions and one on a center of symmetry. One of the hexafluorophosphate counterions in general positions was assigned half-weight occupancy. All non-hydrogen atoms were refined anisotropically. In the case of the [2]catenane **4**·4PF_6, seven of the eight hexafluorophosphate counterions were in general positions and two in special positions with half weight occupancy. All non-hydrogen atoms were refined anisotropically.

General Method for the Determination of the Association Constants by UV−Vis Spectroscopy Employing the Titration Methodology. A series of solutions with constant concentrations (∼10^{-3} M) of the host and containing different amounts of guest (from ∼10^{-4} to 10^{-2} M) in either CD_3CN or Me_2CO were prepared. The absorbance at the wavelength (λ_{max}) corresponding to the maximum of the charge-transfer band for the 1:1 complex was measured for all the solutions at the same temperature T. The correlation between the absorbance and the guest concentration was used[18] to evaluate the association constants (K_a) using a nonlinear curve-fitting program.

General Method for the Determination of the Association Constants by ^{1}H-NMR Spectroscopy Employing the Continuous Variations Methodology. A solution of [BBIPYBIXYCY][PF_6]$_4$ and a solution of the π-electron-rich acyclic guest with identical concentrations (∼10^{-3} M) were prepared using CD_3CN as the solvent. By employing the two stock solutions, several new solutions with the same total volumes, but differing in the ratios of the two components (from 1:9 to 9:1, host:guest), were prepared. The chemical shifts of the protons attached to the hydroquinone ring of the guest were measured by ^{1}H-NMR spectroscopy at the temperature T. The correlation between the mole fraction of the guest and the chemical shift change for the probe protons was used[18] to evaluate the association constant (K_a) in a nonlinear curve-fitting program.

General Method for the Determination of the Kinetic and Thermodynamic Parameters Associated with the Hydrolysis of the [2]Catenanes. A solution of the [2]catenane of known concentration (C_0 = 0.003 mM) in CD_3CN/D_2O (1:1, v/v, 0.5 mL) was heated at 50 °C for *ca.* 1500 h. The reaction was followed by ^{1}H-NMR spectroscopy, and the molar concentration C of the [2]catenane, calculated by integrating the resonances associated with the protons in the α-positions with respect to the nitrogen atoms on the bipyridinium units, was plotted against time (t). Fitting of the data by means of a nonlinear curve-fitting program employing eq 2[19] where C_e is the molar concentration of the [2]catenane at equilibrium, afforded the rate constant (k_{-}) of the hydrolysis reaction.

$$C = C_0 - \frac{C_e\, e^{\frac{k_{-}Ct}{C_e}} - C_e}{e^{\frac{k_{-}Ct}{C_e}}} \qquad (2)$$

Molecular Modeling. The initial structures for the calculations were obtained from the X-ray crystallographic coordinates of the corresponding pseudorotaxane-like complexes. The bond orders were inserted into the structures and counterions and solvent molecules were removed. The resulting files were subjected to single-point calculations using the AM1 Hamiltonian resident within Spartan,[11] with the option for the calculation of the electrostatic surfaces activated. The generation of the points of maximum electrostatic interaction and the creation of the electrostatic iso-surfaces were achieved using the graphic options of Spartan. The two conformations of the model compound, methyl 2-methoxyacetate, were generated within the Spartan builder module and ab initio calculations at the 6-31G*/MP2 level were performed again within Spartan.

Acknowledgment. This research was supported by the Biotechnology and Biological Sciences Research Council, by the Engineering and Physical Sciences Research Council, by the European Community Human Capital and Mobility Programme, and by the Ciba-Geigy Foundation (Japan) for the Promotion of Science.

Supporting Information Available: Figures illustrating (i) the pairs of hydrogen bonding interactions linking adjacent [2]-pseudorotaxanes and [2]catenanes in the crystal and (ii) donor−acceptor stacks propagating along the b crystallographic direction in one of the [2]catenanes and tables listing atomic coordinates, temperature factors, bond lengths and angles, and torsion angles (80 pages). See any current masthead page for ordering and Internet access instructions.

JA962937Z

(18) Connors, K. A. *Binding Constants*; Wiley: New York, 1987.

(19) Laidler, K. J. *Chemical Kinetics*; Harper Collins Publisher: New York, 1987.